Article

H₂O₂-mediated oxidation of PHOSPHATE STARVATION RESPONSE2 promotes adaptation to low phosphate in rice

Funing Meng[1,5], Dan Xiang[1,4,5], Ziqi Bu[2], Rongbin Lin[1], Xinyang Sun[1], Jiming Xu[1], Yunrong Wu [1], Yu Liu[1], Zhongchang Wu[1], Xiaorong Mo[1], Javier Paz-Ares [3] & Chuanzao Mao [1,2] ✉

Phosphorus (P) is an essential macro-nutrient for plant growth and development. It is preferentially taken as inorganic phosphate (Pi). Plants have evolved elaborate mechanisms to adapt to low Pi (LP) stress through activating Pi-starvation responses. H_2O_2 is an important signal molecule involved in plant adaptation to diverse environmental stresses. However, whether H_2O_2 plays a role in Pi-starvation responses remains unknown. Here, we reveal that H_2O_2 produced by the respiratory burst oxidase homologs OsRBOH-D/H facilitates phosphate uptake and utilization under LP conditions in rice. Mechanistically LP-induced H_2O_2 promotes the oxidization of the key phosphate signaling transcription factor PHOSPHATE STARVATION RESPONSE2 (OsPHR2) at its Cys377 residue to trigger its oligomerization, sequence-specific DNA binding ability, and nuclear translocation, thereby activating Pi-starvation responses to adapt to LP conditions. Additionally, our molecular and biochemical data revealed that *OsRBOH-D* is a direct target gene of OsPHR2. Thus, OsPHR2 and OsRBOH-D form a positive feedback regulatory loop in which H_2O_2 acts as a second messenger to amplify the Pi-starvation response.

Phosphorus (P) is an essential macronutrient for plant growth and development. Although P is abundant in soil, inorganic phosphate (Pi), the plant-absorbable form of P, easily forms insoluble precipitates with organic matter or mineral cations, resulting in low Pi (LP) availability in soil[1–4]. Pi deficiency restricts plant growth, and to improve crop yields, large quantities of P fertilizer have been applied in agricultural production, which increases the agricultural costs, aggravates environmental pollution, as well as depletes the non-renewable phosphate rock reserves for phosphorus fertilizer production[4–9]. Rice (*Oryza sativa*), one of the most staple cereal crops worldwide, feeds more than half of the global population[10]. Breeding P efficient rice varieties is an effective approach for agricultural sustainability, which requires a

deeper understanding of the regulatory mechanisms of low-phosphate tolerance.

Plants have evolved an effective rescue system, formed by an array of Pi-starvation responses involving transcriptional reprogramming, morphological remodeling, and increased Pi acquisition, remobilization, redistribution and utilization to cope with Pi deficiency[11–15]. A subclade of the myeloblastosis (MYB) transcription factors, such as PHOSPHATE STARVATION RESPONSE1 (AtPHR1) in *Arabidopsis* and OsPHR2 in rice, have been shown to be a central regulator of Pi-starvation responses. OsPHR2 activates Pi acquisition, translocation and redistribution through three regulatory pathways: (1) OsPHR2 positively regulates *OsIPS1* (a noncoding RNA) and *OsmiR399* to

---

[1]State Key Laboratory of Plant Environmental Resilience, College of Life Sciences, Zhejiang University, Hangzhou, China. [2]Hainan Institute, Zhejiang University, Yazhou Bay Science and Technology City, Sanya, Hainan, China. [3]Department of Plant Molecular Genetics, Centro Nacional de Biotecnologia-Consejo Superior de Investigaciones Cientificas, Madrid, Spain. [4]Present address: Institute of Nuclear Agricultural Sciences, Key Laboratory of Nuclear Agricultural Sciences of Ministry of Agriculture and Zhejiang Province, College of Agriculture and Biotechnology, Zhejiang University, Hangzhou, China. [5]These authors contributed equally: Funing Meng, Dan Xiang. ✉e-mail: mcz@zju.edu.cn

coordinate the expression level of *OsPHO2*, which encodes an ubiquitin-conjugating E2 enzyme responsible for the stability of OsPHO1, thus mediating Pi efflux into the root xylem vessel and translocation to the shoot[16]; (2) OsPHR2 positively regulates *OsmiR827* for cleavage of two target genes *OsSPX-MFS1* and *OsSPX-MFS2*, which involves in Pi transport into the vacuole to maintain Pi homeostasis[17]; and (3) OsPHR2 directly upregulates *OsPT*s, encoding Pi transporters, to promote Pi uptake from rhizosphere and root-to-shoot Pi translocation[18].

The function of OsPHR2 is negatively regulated by OsSPX1-OsSPX6[19–24], proteins exclusively harboring the SPX (SYG1, Pho81, and XPR1) domain[25], which act as sensors of inositol pyrophosphates (IP). Under Pi-sufficient conditions, where IP levels are high, the formation of OsPHR2-IPs-OsSPX4 complex prevents OsPHR2 translocation into the nucleus, while in the nucleus, other OsSPX proteins interact with OsPHR2, thereby inhibiting its function and consequently limiting the expression of PSI genes. Under Pi-deficient conditions, the levels of intracellular IPs decrease, which results in the dissociation of OsPHR2-IPs-OsSPX4 followed by the ubiquitination-mediated degradation of OsSPX4 and OsSPX6, releasing OsPHR2 into the nucleus to bind to the P1BS element in the promoter of PSI genes, consequently inducing their expression and leading to activation of the Pi-starvation responses[19–24]. In addition, the E3 ubiquitin ligase HAEMERYTHRIN MOTIF-CONTAINING REALLY INTERESTING NEW GENE (RING) AND ZINC-FINGER PROTEIN1/2 (OsHRZ1/2) interacts with OsPHR2 to promote its degradation, coordinating phosphorus-iron homeostasis[26]. Another mechanism of negative regulation of OsPHR2 involves glycogen synthase kinase 3 (GSK3)-like protein OsGSK2 that phosphorylates OsPHR2 at its Ser269 residue. Such phosphorylation impairs OsPHR2 DNA-binding ability to restrict the expression of *PSI* genes and reduce Pi acquisition[27]. In *Arabidopsis*, AtSIZ1-mediated AtPHR1 sumoylation is crucial for its stability to regulate Pi starvation-responsive genes[28]. These results imply that posttranslational modifications (PTMs) are critical for PHR transcription factor activity. However, whether the function of OsPHR2 is regulated by additional PTMs awaits further investigation.

Reactive oxygen species (ROS) are recently recognized as important signal molecules that regulate growth and development, as well as stress responses in plants and animals[29]. There are mainly four kinds of ROS, namely superoxide anion ($O_2^{·-}$), hydrogen peroxide (H_2O_2), singlet oxygen ($^1O_2$), and hydroxyl radical (·OH)[30]. Compared with other ROS, H_2O_2 can function as an important signal molecule given its specific physical (a remarkable long half-time, $>10^{-3}$ s) and chemical (rapid and reversible oxidation of target proteins) properties[30,31]. Previous studies have proposed that H_2O_2 can cause oxidation of thiol groups of cysteine in target proteins, which either activates, inactivates, or alters their conformations and functions to affect diverse signaling pathways[31]. In plants, H_2O_2 plays an important role in regulating growth and development[32–37], as well as responses to stresses, such as saline-alkali, drought, cold, and heat[38–41]. For example, salt-induced H_2O_2 coordinates plant growth and stress responses by sulfenylating TRYPTOPHAN SYNTHASE B SUBUNIT 1 (AtTSB1) and plastid TRIOSE PHOSPHATE ISOMERASE (pdTPI), triggering repression of plant growth and enhancement of salt stress tolerance[38]; the redox-sensitive protein, OsGPX1, can be oxidized by drought-induced H_2O_2 to form disulfide bond between Cys71 and Cys90, which facilitates its nuclear translocation to interact with and oxidize the transcription factor basic LEUCINE ZIPPER 68 (OsbZIP68) at its Cys245 residue, causing OsbZIP68 to form a homotetramer with higher transcriptional activation activity towards osmotic-responsive genes, conferring plant tolerance to osmotic stress[39]; likewise, upon high-temperature stress, H_2O_2 mediates the oxidation of heat shock transcription factors AtHSFA8 and AtHSFA1a to enhance their transcriptional activation of heat-induced genes, thus facilitating the heat stress response and tolerance[40]. The cold stress-induced H_2O_2 promotes

ENOLASE 2 (AtENO2) oligomerization and translocation into the nucleus, where the oxidized AtENO2 binds to the promoter of *AtCBF1* and activates its expression to facilitate the expression of *AtCOR* genes, thus promoting plant cold stress tolerance[41]. ROS are generated in diverse cellular compartments in plants, such as chloroplasts, mitochondria, plasma membrane, cell wall, apoplast, cytosol, peroxisome, glyoxysome, or endoplasmic reticulum. The generation of ROS in different compartments from multiple pathways depends on the plant tissue, developmental stage, and external conditions. It was reported that the respiratory burst oxidase homologs (RBOH) in the apoplast are involved in the generation of H_2O_2 in response to environmental stresses[42,43]. AtRBOH-C regulates root hair formation and mechanosensing[44,45]. AtRBOH-D mediates many processes such as pathogen responses, stomatal closure, systemic signaling in response to abiotic stresses or lignification[46–51]. There is evidence for functional redundancy among RBOHs, for example, the double mutant *rboh-D/rboh-F* shows enhanced phenotypes compared to the individual mutants in pathogen response, cell death regulation, or stomatal closure in *Arabidopsis*[46,47,52]. Studies have shown that the activity of AtRBOH-D is regulated by different mechanisms, such as, N-terminal phosphorylation, C-terminal phosphorylation and ubiquitination, extracellular ATP, and S-nitrosylation[43,45–47,52]. Although RBOHs-stimulated changes in gene expression are essential for diverse plant developmental processes and environmental responses, the involvement of RBOHs in regulating Pi-starvation responses remains unknown[53,54].

In this study, we examine the involvement of H_2O_2 in phosphate starvation signaling and demonstrate that LP triggers H_2O_2 production involving the respiratory burst oxidase homologs RBOH-D and H, which play a crucial role in promoting rice adaptation to LP. We show that H_2O_2 facilitates oxidation of OsPHR2Cys377 to promote its oligomerization, enhances its nuclear translocation and DNA binding ability to the promoters of PSI genes. Our study reveals a hitherto unidentified positive regulatory loop formed by OsPHR2 and RBOH-D/H that results in amplification of the Pi starvation response to promote adaptation to LP environments in rice.

Results

H_2O_2 production mediated by OsRBOH-D/H promotes rice adaptation to LP

To determine whether H_2O_2 is involved in activating Pi-starvation responses to cope with Pi limitation, we first examined H_2O_2 levels in the shoot and root of 7-day-old wild-type XS134 plants grown hydroponically under low Pi (LP; $10\,\mu M\ KH_2PO_4$) or high Pi (HP; $200\,\mu M\ KH_2PO_4$) conditions. Results showed that H_2O_2 levels in shoot and root were significantly increased under LP treatment for 2 days compared to normal growth conditions (Fig. 1a and Supplementary Fig. 1a). We next examined the effect of H_2O_2 on PSI gene expression. Reverse transcription quantitative polymerase chain reaction (RT-qPCR) analysis indicated that the expression levels of PSI genes, e.g., *OsIPS1*, *OsPT10*, *OsSPX1* and *OsmiR827*, were clearly induced after H_2O_2 treatment for 1 or 2 h, and this effect was suppressed after treatment with H_2O_2 scavenger potassium iodide (KI) (Supplementary Fig. 1b, c). Subsequently, we investigated the growth performance of 7-day-old XS134 plants treated with different concentrations of H_2O_2 or KI under HP or LP conditions for 28 days. Shoot and root Pi concentrations were significantly increased after 1−5 mM H_2O_2 treatment, while plant growth was promoted at 1−2 mM H_2O_2 treatment under both HP and LP conditions, and the PSI genes were induced significantly by exogenous H_2O_2 treatment (Fig. 1b–f; Supplementary Figs. 2a, c–e, 3). Conversely, KI treatment significantly inhibited rice growth, decreased Pi contents under both HP and LP conditions, and suppressed the expression response of PSI genes to LP (Fig. 1f; Supplementary Figs. 2b, f–h; Supplementary Fig. 3). These results suggest that H_2O_2 is involved in plant adaption to Pi deficiency in rice; furthermore, suitable
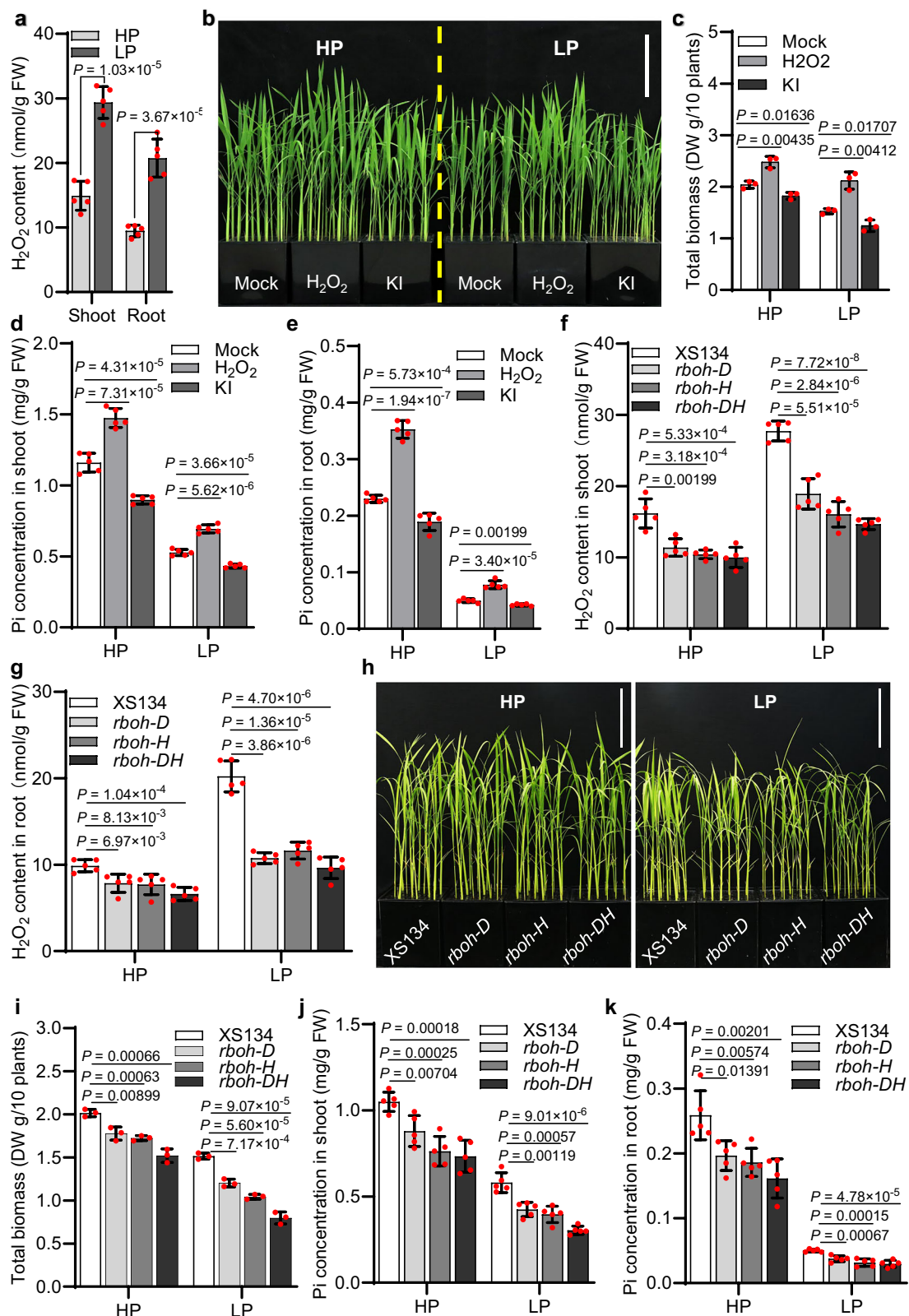
Fig. 1 | H₂O₂ promotes Pi acquisition and signaling in rice. a The H₂O₂ content in the shoot and root of 7-day-old wild type XS134 plants cultured hydroponically under HP or LP conditions for 2 days. **b–e**, The morphology (**b**), biomass (**c**), and Pi concentrations in shoot (**d**) and in root (**e**) of wild type XS134 plants treated with 1 mM of H₂O₂ or 10 μM KI cultured hydroponically under HP or LP conditions for 28 days. **f**, **g** The H₂O₂ content in shoot (**f**) and root (**g**) of the 7-day-old wild type XS134, *rboh-D*, *rboh-H*, and *rboh-DH* plants cultured hydroponically under HP or LP conditions for an additional 2 days. **h–k** The morphology (**h**), biomass (**i**) and Pi concentrations in shoot (**j**) and root (**k**) of wild type XS134, *rboh-D*, *rboh-H*, and double mutant *rboh-DH* plants cultured hydroponically for 28 days under HP or LP conditions. Bar = 10 cm in **b** and **g**. DW dry weight, FW fresh weight. Data are means ± SD (*n* = 5 replicates, 3 seedlings per replicate for **a**, **d**, **e**, **f**, **g**, **j**, and **k**; *n* = 3 replicates, 10 seedlings per replicate for **c** and **i**). The *P*-value was generated by a two-sided Student's *t* test. Source data are provided in the Source Data file.

concentrations of exogenous H_2O_2 treatment significantly promotes Pi acquisition and plant growth in rice.

The implication of RBOHs in the generation of H_2O_2 in response to several environmental stresses[42,43] prompted us to investigate their possible roles in LP-induced H_2O_2. We examined the expression of all nine rice *OsRBOH* genes in response to LP treatment. We found that *OsRBOH-D* and *OsRBOH-H* were induced dramatically after LP treatment for 2 days in both shoot and root, while the expression of the other *OsRBOHs* were not obviously changed (Supplementary Fig. 4a, b). Further analysis revealed that both *OsRBOH-D* and *OsRBOH-H* are expressed in root, stem, leaf and leaf sheath and root shoot junction (Supplementary Fig. 4c). Then we generated *rboh-D* and *rboh-H* single mutants and double mutant *rboh-DH* using CRISPR/Cas9 genome editing system to examine whether *OsRBOH-D* and *OsRBOH-H* are involved in LP-induced H_2O_2 production (Supplementary Fig. 5). Results showed that the LP-induced H_2O_2 accumulation was significantly suppressed in both single mutants (*rboh-D* or *rboh-H*) and double mutant (*rboh-DH*) (Fig. 1g and Supplementary Fig. 6). Phenotypic analysis revealed that *rboh-D*, *rboh-H* and *rboh-DH* mutants displayed lower biomass and Pi concentrations compared with that of the wild type XS134 under HP or LP conditions, and the expression response of PSI genes to LP treatment was significantly compromised in *rboh-D*, *rboh-H* and *rboh-DH* mutants (Fig. 1h–k and Supplementary Fig. 7). These results suggest that OsRBOH-D/H are involved in LP-induced H_2O_2 production in rice.

H_2O_2 oxidizes OsPHR2 to facilitate LP adaptation in rice

H_2O_2 usually participates in the post-translational modification (PTM) of oxidizing thiols (-SH) into sulfenic acid (-SOH) in the cysteine (Cys) residues of target proteins[55]. A previous study showed that biotin conjugated iodoacetamide (BIAM) and H_2O_2 could selectively and competitively react with cysteine residues that exhibit a low pKa in target proteins; thus, the H_2O_2-sensitive and H_2O_2-oxidized cysteine residues can be detected by BIAM-labeling and biotin-switch assays, respectively[56] (Fig. 2a, b). Given the central role of OsPHR2 in regulating Pi-starvation responses in rice, we examined whether H_2O_2 induces oxidation of OsPHR2 using these BIAM-labeling and biotin-switch assays. Towards this, maltose-binding protein (MBP) and MBP-OsPHR2 were pretreated with or without H_2O_2, and then incubated with BIAM. Results showed that MBP-OsPHR2, but not the MBP control, was labeled by BIAM, and the labeling levels were decreased by H_2O_2 treatment in a dose-dependent manner (Fig. 2c), indicating that H_2O_2 decreased the reduced form of cysteine residues of OsPHR2. To further detect the cysteine oxidation of OsPHR2, the H_2O_2-treated MBP-OsPHR2 was first incubated with a thiol alkylation reagent, N-ethylmaleimide (NEM), which irreversibly modifies free thiols in proteins. The NEM-modified MBP-OsPHR2 was then precipitated, treated with DTT to reduce any oxidized cysteines pre-existing before NEM treatment. The newly exposed free thiol groups were then labeled with BIAM. The BIAM-tagged proteins in the samples were then immunoprecipitated with streptavidin beads and revealed by western blot analysis. The results showed that H_2O_2 promotes oxidation of OsPHR2 in a dose-dependent manner in vitro (Fig. 2c).

Then, we assayed the OsPHR2 oxidation in H_2O_2- and LP-treated 7-day-old rice. Compared with untreated rice plants, both H_2O_2 and LP-treated OsPHR2-mCherry/XS134 transgenic plants displayed significantly increased levels of OsPHR2 oxidation. However, the H_2O_2 treatment but not the LP treatment significantly increased the levels of OsPHR2 oxidation in OsPHR2-mCherry/*rboh-DH* transgenic plants (Fig. 2d), suggesting that RBOH-D/H mediate LP-induced oxidation of OsPHR2 in rice. Then we generated a *phr2* mutant using the CRISPR/Cas9 genome editing system (Supplementary Fig. 8a, b) to explore whether OsPHR2 is involved in H_2O_2-promoted Pi-starvation responses. Results showed that the LP-induced H_2O_2 accumulation was significantly suppressed in *phr2* mutant (Supplementary Fig. 8c, d). The

phr2 mutant was smaller and had lower shoot and root Pi concentrations than that of XS134 under HP or LP conditions (Fig. 2e–h). Moreover, the H_2O_2-promoted increase in biomass, Pi concentration in shoot and root under both HP and LP conditions, and the LP induced upregulation of PSI genes were compromised in *phr2* compared with that in XS134 (Fig. 2e–h and Supplementary Fig. 9). This result indicates that OsPHR2 is essential for H_2O_2-promoted LP adaptation in rice, and that the residual responsiveness in *phr2* probably reflect the action of partially redundant OsPHR2 homologs[27].

Cys377 is the main target of H_2O_2 mediated oxidation at OsPHR2 under Pi-deficiency

To determine which cysteine (Cys, C) residue of OsPHR2 is oxidized by H_2O_2, we generated and purified four mutated OsPHR2 variants, namely OsPHR2 C140S (hereafter C140S), C195S, C368S, or C377S, by mutating the C140, C195, C368, or C377 residue individually to serine (Ser, S) residue, as OsPHR2 contains only four Cys residues (Fig. 3a). Then, we treated these four MBP fusion OsPHR2 variants with 5 mM H_2O_2 to examine their oxidation level. We found that the oxidation level of MBP-C140S, MBP-C195S, or MBP-C368S was similar as that of the wild type MBP-OsPHR2, whereas the oxidation level in MBP-C377S was dramatically reduced (Fig. 3a), suggesting that Cys377, located in the coiled coil (CC) dimerization domain of OsPHR2 (Fig. 3a), is critical for the H_2O_2-mediated OsPHR2 oxidation. To investigate its oxidation in vitro, we separately transformed OsPHR2-GFP, OsPHR2C140S-GFP (hereafter C140S-GFP), and C377S-GFP into *phr2* and treated these transgenic plants with LP or 2 mM H_2O_2 for 2 days. Western blotting results showed that the oxidation variant in OsPHR2-GFP/*phr2* or C140S-GFP/*phr2* was increased by LP or H_2O_2 treatment, whereas the oxidation variant was not detected in C377S-GFP/*phr2* plants, even after LP or H_2O_2 treatments (Fig. 3b). Total levels of GFP-PHR2 and variants were similar, excluding protein instability of C377S-GFP which would result in the no detection of the oxidation variant. These findings verified the essential role of Cys377 in H_2O_2-mediated OsPHR2 oxidation under Pi-deficiency in rice.

After cultured under HP or LP conditions for 28 days, the growth performance of OsPHR2-GFP/*phr2* and C140S-GFP/*phr2* transgenic plants were comparable with that of wild type XS134 with slightly higher biomass, Pi concentration and up-regulation of PSI genes in response to LP, while the C377S-GFP/*phr2* plants were almost like *phr2* in growth performance, biomass, Pi concentration and the up-regulation of PSI genes in response to LP (Fig. 3c–f and Supplementary Fig. 10). Altogether, these results indicate that Cys377 is essential for OsPHR2 function and is the primary target of LP-induced H_2O_2 oxidation of OsPHR2.

LP-promoted OsPHR2 oxidation enhances its nuclear translocation and DNA-binding ability

To understand how the LP-promoted oxidation of OsPHR2 affects its function, we first examined whether oxidation of OsPHR2 affects its nuclear localization by transiently expressing OsPHR2 and its mutated variants fused with GFP in *N. benthamiana* leaves. Results showed that under mock conditions, OsPHR2-GFP, C140S-GFP, C195S-GFP and C368S-GFP were preferentially localized in the nucleus, with some GFP signal detected in the cytoplasm, whereas C377S-GFP was preferentially localized in the cytoplasm (Fig. 4a, b). Compared with mock conditions, the accumulation of OsPHR2-GFP, C140S-GFP, C195S-GFP and C368S-GFP in the nucleus were increased significantly after H_2O_2 or LP treatment. In contrast, the level of C377S-GFP in the nucleus was practically unchanged after H_2O_2 or LP treatment (Fig. 4a, b). Similarly, both LP and H_2O_2 treatments triggered nuclear translocation of OsPHR2-GFP and C140S-GFP, but not C377S-GFP in transgenic plants stably expressing OsPHR2-GFP, C140S-GFP and C377S-GFP, respectively (Fig. 4c, d). These results suggest that Cys377 is essential for the proper nuclear translocation of OsPHR2 in response to Pi-deficiency.
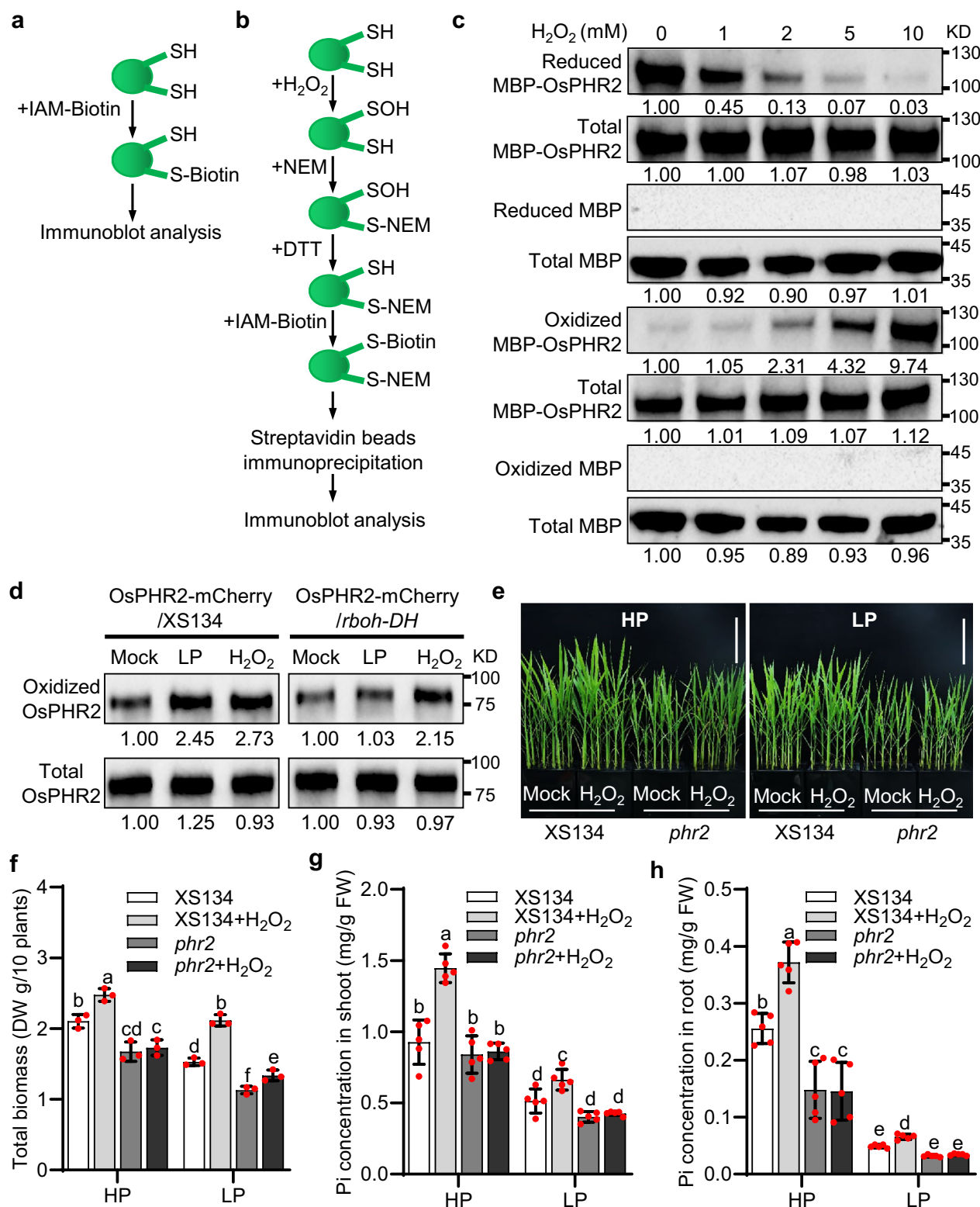
Fig. 2 | OsPHR2 is oxidized by H_2O_2. a, **b** The flowcharts show the procedures for quantifying redox modification of target proteins by BIAM-labeling assay (**a**) and biotin-switch assay (**b**). **c** In vitro analysis of the reduction and oxidation of OsPHR2 under H_2O_2 treatment through BIAM-labeling assay (upper panel) and biotin switch assay (lower panel) using anti-MBP antibody. **d** Analysis of oxidation of OsPHR2 in transgenic rice. Total proteins were extracted from 7-day-old indicated plants treated with 2 mM H_2O_2 or LP for an additional 2 days and then subjected to biotin switch assay using anti-mCherry antibody. **e**–**h** The morphology (**e**), biomass (**f**), Pi concentrations in shoot (**g**) and root (**h**) of wild type XS134 and *phr2* plants treated with or without 1 mM H_2O_2 cultured hydroponically under HP or LP conditions for 28 days. Bar = 10 cm in **e**; DW dry weight, FW fresh weight. The immunoblot analysis was repeated three times with similar results for **c** and **d**. Data are means ± SD (n = 3 replicates, 10 seedlings per replicate for **f**; n = 5 replicates, 3 seedlings per replicate for **g** and **h**). The different letters above the bars denote significant differences ($P < 0.05$) according to a two-sided Duncan's multiple range test for **f**–**h**. Source data are provided in the Source Data file.
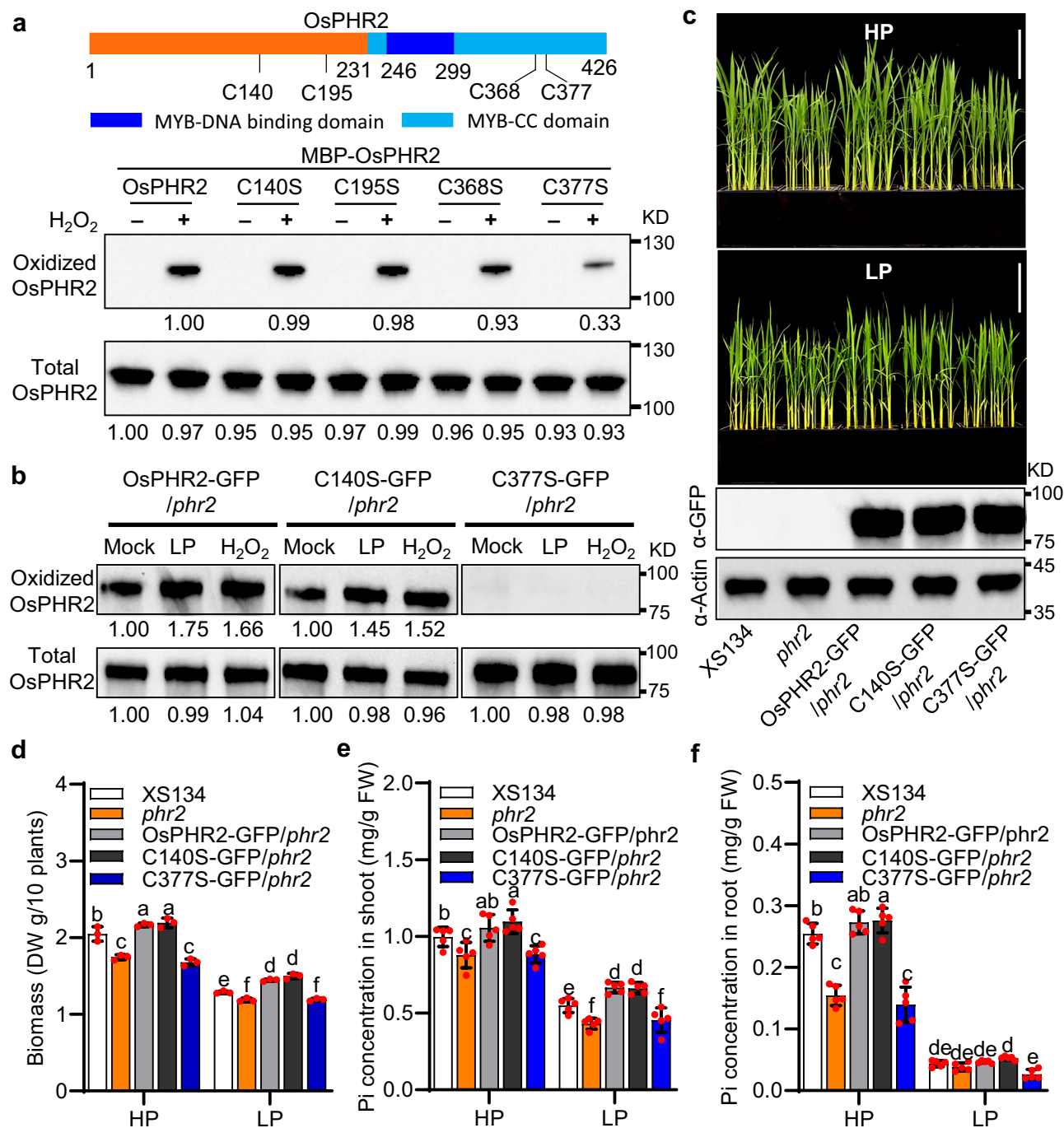
Fig. 3 | H₂O₂-mediated OsPHR2 Cys377 oxidation is critical for promoting Pi-starvation responses in rice. a In vitro analysis of the oxidation of OsPHR2 and its mutated variants. The MBP-OsPHR2 and its mutated variants pretreated with 0 or 5 mM H₂O₂ for 30 min were subjected to biotin switch assay using anti-MBP antibody. **b** Analysis of oxidation of OsPHR2 and its mutated variants in rice. Total proteins were extracted from 7-day-old OsPHR2-GFP/*phr2*, C140S-GFP/*phr2*, and C377S-GFP/*phr2* plants treated with 2 mM H₂O₂ or LP for 2 days and then subjected to biotin switch assay using anti-GFP antibody. **c-f** The morphology (**c**), biomass

(**d**), Pi concentrations in shoot (**e**) and root (**f**) of wild type XS134, *phr2*, OsPHR2-GFP/*phr2*, C140S-GFP/*phr2*, and C377S-GFP/*phr2* plants cultured hydroponically under HP or LP conditions for 28 days. Bar = 10 cm in **c**; DW dry weight, FW fresh weight. The immunoblot analysis was repeated three times with similar results for **a-c**. Data are means ± SD (*n* = 3 replicates, 10 seedlings per replicate for **d**; *n* = 5 replicates, 3 seedlings per replicate for **e** and **f**). The different letters above the bars denote significant differences (*P* < 0.05) according to a two-sided Duncan's multiple range test for **d-f**. Source data are provided in the Source Data file.

To further verify this finding, we assayed the protein levels of OsPHR2 variants in the cytosolic and nuclear fractions of H₂O₂- or LP-treated transgenic plants. Results showed that in OsPHR2-GFP/*phr2* transgenic plants treated with H₂O₂ or LP, OsPHR2-GFP protein accumulated more in the nucleus and less in the cytoplasm compared to mock-treated plants (Fig. 4e), suggesting that H₂O₂ or LP facilitates the

nuclear localization of OsPHR2. Furthermore, LP-induced OsPHR2 nuclear translocation was compromised in OsPHR2-GFP/*rboh-DH* plants compared with that in OsPHR2-GFP/*phr2* plants, while H₂O₂-induced OsPHR2-GFP nuclear translocation was comparable between OsPHR2-GFP/*rboh-DH* and OsPHR2-GFP/*phr2* plants (Fig. 4e), indicating that RBOH-D/H-mediated production of H₂O₂ facilitates OsPHR2
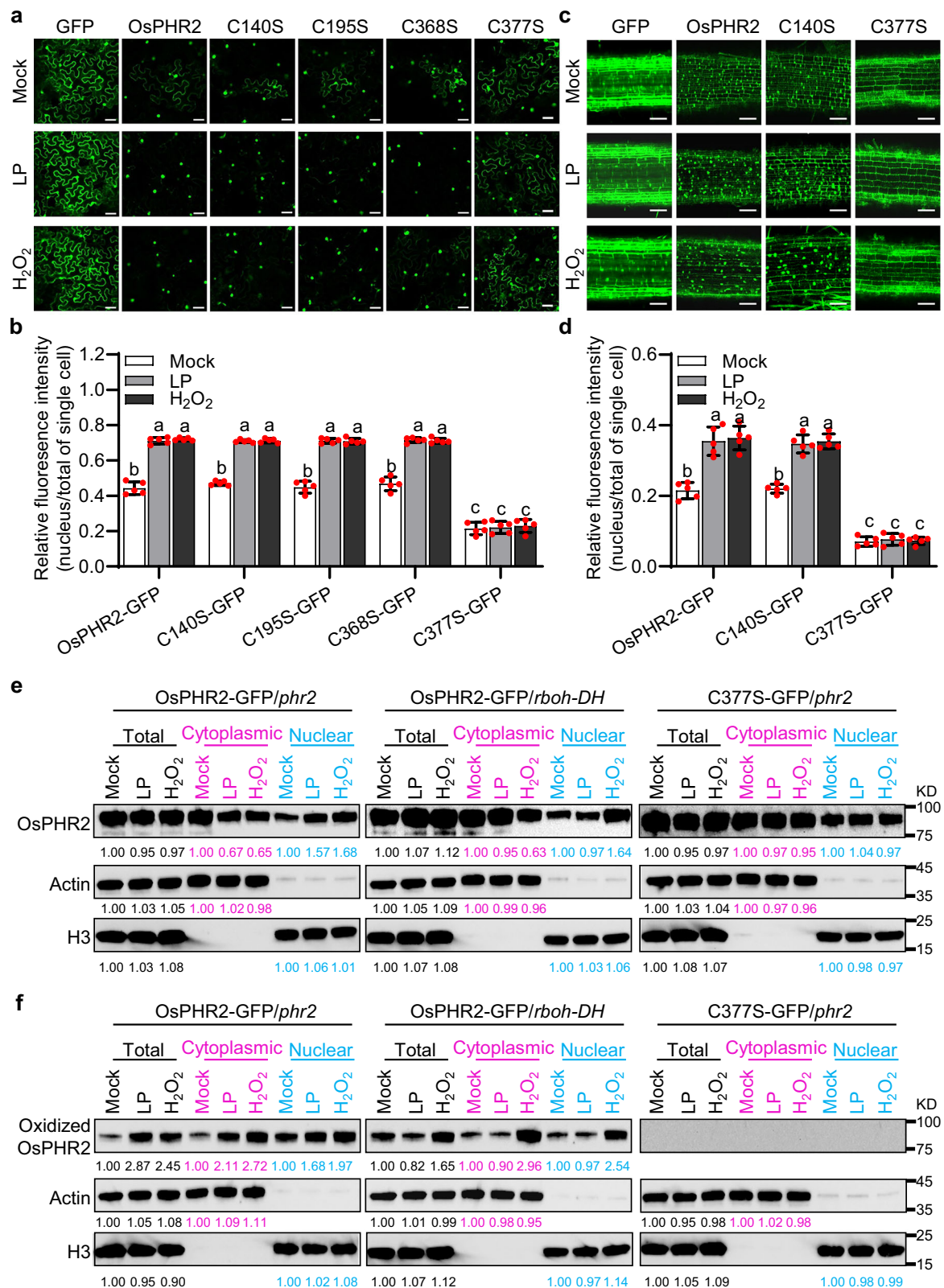
nuclear translocation in response to Pi-deficiency. Consistent with this result, oxidized OsPHR2-GFP was markedly increased in nucleus and cytoplasm by LP treatment in OsPHR2-GFP/*phr2* but not in OsPHR2-GFP/*rboh-DH* plants, while the oxidized OsPHR2-GFP was increased in nucleus and cytoplasm by H₂O₂ treatment in both OsPHR2-GFP/*phr2* and OsPHR2-GFP/*rboh-DH* transgenic plants (Fig. 4f). In addition, our cell fractionation assays further revealed that in C377S-GFP/*phr2*

transgenic plants, but not in C140S-GFP/*phr2* transgenic plants, the localization of OsPHR2 in nucleus and cytoplasm was not changed by either H₂O₂ or LP treatment (Fig. 4e and Supplementary Fig. 11). Consistently, we did not detect the oxidized OsPHR2 in C377S-GFP/*phr2* transgenic plants, which was detected in C140S-GFP/*phr2* transgenic plants, under either H₂O₂ or LP treatments (Fig. 4f and Supplementary Fig. 11). These results further support the notion that H₂O₂-mediated

Fig. 4 | LP-induced H₂O₂ promotes OsPHR2 nuclear translocation. a The subcellular localization of OsPHR2 and its mutated variants under LP or H₂O₂ treatment. OsPHR2-GFP, C140S-GFP, C195S-GFP, C368S-GFP and C377S-GFP were transiently expressed in leaves of *N. benthamiana* plants pretreated with 2 mM H₂O₂ or LP for 2 days. After 2 days of growth in darkness, the GFP fluorescence signal was detected using confocal laser scanning microscopy. Bar = 50 μm. **b** The relative nuclear fluorescence intensity/total fluorescence intensity within cells indicated in (**a**). **c** The subcellular localization of OsPHR2, C140S, and C377S in transgenic rice root. Seven-day-old 35S::OsPHR2-GFP/*phr2*, 35S::C140S-GFP/*phr2*, and 35S::C377S-GFP/*phr2* plants were treated with 2 mM H₂O₂ or LP for an additional 2 days, then the GFP fluorescence signal in epidermal cells of the primary root maturation zone was detected using confocal laser scanning microscopy. Bar = 100 μm. **d** The relative nuclear fluorescence intensity/total fluorescence intensity within cells indicated in (**c**). **e, f** Immunoblot analysis of the accumulation of OsPHR2 (**e**) and oxidation of OsPHR2 (**f**) in nucleus and cytoplasm in 35S::OsPHR2-GFP/*phr2*, 35S::OsPHR2-GFP/*rboh-DH* and 35S::C377S-GFP/*phr2* plants. For OsPHR2 accumulation analysis, the 7-day-old plants were treated with 2 mM H₂O₂ or LP for additional 2 days and then used to isolate total, cytoplasmic, and nuclear proteins and then subjected to immune blot analysis using anti-GFP antibody; for OsPHR2 oxidation analysis, the total, cytoplasmic, and nuclear proteins were isolated from 7-day-old indicated plants treated with 2 mM H₂O₂ or LP for additional 2 days and then subjected to biotin switch assay using anti-GFP antibody. Histone3 (H3) was used as the loading control for nuclear proteins, and Actin was used as the loading control for total and cytoplasmic proteins in (**e** and **f**). The relative intensity of nuclear OsPHR2-GFP proteins were normalized to H3, while the total (or cytoplasmic) OsPHR2-GFP proteins were normalized to Actin, the mock treatment was set to 1. The immunoblot analysis was repeated three times with similar results for **e** and **f**. Data are means ± SD (n = 5 replicates for **b** and **d**). The different letters above the bars denote significant differences ($P < 0.05$) according to a two-sided Duncan's multiple range test. Source data are provided in the Source Data file.

OsPHR2 Cys377 oxidation promotes its nuclear translocation under Pi-deficiency.

We also examined whether LP or H₂O₂ treatment affects OsPHR2 binding ability to target gene promoters using a dual-luciferase (LUC) reporter system (Fig. 5a, b). Results showed that OsPHR2-GFP and C140S-GFP prompted the expression of LUC reporters driven by *OsIPS1*, *OsSPX1*, or *OsmiR827* promoters, which was considerably enhanced by H₂O₂ or LP treatment, whereas the transcriptional activation effect of C377S was much weaker and not significantly changed by H₂O₂ or LP treatment (Fig. 5c). In addition, we performed a ChIP-qPCR assay using GFP/*phr2*, GFP/*phr2 rboh-DH*, OsPHR2-GFP/*phr2*, OsPHR2-GFP/*phr2 rboh-DH*, C140S-GFP/*phr2*, C377S-GFP/*phr2* transgenic plants. Results showed that OsPHR2-GFP and C140S-GFP bind *in planta* to *OsIPS1*, *OsSPX1*, and *OsmiR827* promoters with a similar strength, however, the binding of C377S-GFP to these promoters is clearly much weaker. Moreover, the binding of OsPHR2-GFP and C140S-GFP *in planta* to these target promoters was increased by LP or H₂O₂ treatment, while the LP or H₂O₂ treatments had no effect on C377S-GFP binding to target promoters (Fig. 5d and Supplementary Fig. 12a). In addition, the LP-promoted but not H₂O₂-promoted enrichment of OsPHR2 binding to the *OsIPS1*, *OsSPX1*, or *OsmiR827* promoter was significantly reduced in OsPHR2-GFP/*phr2 rboh-DH* transgenic plants (Fig. 5d and Supplementary Fig. 12a). In order to verify whether the oxidation of Cys377 in OsPHR2 could directly affect its binding ability to DNA in vitro, we performed EMSA experiments using MBP-OsPHR2 and MBP-C377S under different concentrations of H₂O₂ treatments. The results showed that H₂O₂-treated MBP-OsPHR2 displayed greater binding ability than the untreated protein to the *OsIPS1*, *OsSPX1* and *OsmiR827* promoters, while mutation of OsPHR2 at Cys377 dramatically disrupted its DNA-binding ability both in presence and in absence of H₂O₂ (Fig. 5e and Supplementary Fig. 12b). All these findings indicate that H₂O₂-mediated oxidation of OsPHR2 Cys377 enhance its DNA-binding affinity to the promoters of PSI genes, such as *OsIPS1*, *OsSPX1* and *OsmiR827* under Pi-deficiency.

## LP-induced H₂O₂ triggers OsPHR2 oligomerization

Given that Cys377 is located at the CC domain of OsPHR2 and its mutation disrupted OsPHR2 DNA-binding ability, it is possible that oxidation of OsPHR2 Cys377 affects its oligomerization. Yeast two-hybrid assays showed that the interaction between AD-OsPHR2 and BD-OsPHR2 was attenuated by the mutation of C377S but not by other mutations (Supplementary Fig. 13a). Furthermore, H₂O₂ treatment enhanced the interaction intensity between AD-OsPHR2 and BD-OsPHR2, but not between AD-C377S and BD-C377S (Supplementary Fig. 13b), suggesting that Cys377 is essential for the OsPHR2 oligomerization. Moreover, the bimolecular fluorescence complementation (BiFC) assay also showed that the nuclear GFP fluorescence in *N. benthamiana* leaves co-expressing OsPHR2-YFP^N + OsPHR2-YFP^C could be

significantly enhanced by H₂O₂ or LP treatment, and similar results were observed in leaves co-expressing C140S-YFP^N + C140S-YFP^C, C195S-YFP^N + C195S-YFP^C or C368S-YFP^N + C368S-YFP^C. However, the nuclear GFP fluorescence signal was significantly compromised by the C377S mutation and was not affected by H₂O₂ or LP treatment (Fig. 6a, b). These data indicate that OsPHR2 can form oligomers and that Cys377 is essential for this oxidation-mediated oligomerization.

We next examined whether oligomerization of OsPHR2 directly involves disulfide bond formation through Cys377. Towards this, we performed non-reducing SDS-PAGE, in which the intermolecular hydrogen bonds but not disulfide bonds were broken, using proteins extracted from transgenic plants expressing OsPHR2-GFP and its variants in the *phr2* background. Results showed that under non-reducing or denaturing conditions, the dimmers or monomers were detected for OsPHR2-GFP, but less proportion of dimers of OsPHR2-GFP was detected in C377S-GFP/*phr2* transgenic plants under non-reducing conditions, compared with that in OsPHR2-GFP/*phr2*, C140S-GFP/*phr2*, C195S-GFP/*phr2*, and C368S-GFP/*phr2* transgenic plants (Supplementary Fig. 14a, c). In addition, the OsPHR2-GFP dimers were broken down into monomers in non-reducing SDS-PAGE by adding the reducing reagent DL-dithiothreitol (DTT) (Supplementary Fig. 14b), suggesting that the oligomerization of OsPHR2 is maintained by intermolecular disulfide bonds. We further examined the effect of LP or H₂O₂ treatment on the OsPHR2 oligomerization and found that in a non-reducing SDS-PAGE gel, the abundance of OsPHR2-GFP dimers increased under each of these treatments in OsPHR2-GFP/*phr2* transgenic plants (Fig. 6c–e). Similar results were observed for the C140S-GFP variant in C140S-GFP/*phr2* transgenic plants, whereas a much lower proportion of dimers were detected for the C377S-GFP variant in C377S-GFP/*phr2* transgenic plants, which was greatly insensitive to LP and H₂O₂ treatments (Fig. 6c–e). These results suggest that H₂O₂-induced OsPHR2 oligomerization requires Cys377 and involves intermolecular disulfide bond formation.

OsRBOH-D is a direct target gene of OsPHR2

As the expression of *OsRBOH-D* and *OsRBOH-H* were induced under LP treatment, it is possible that *OsRBOH-D* and *OsRBOH-H* are regulated by OsPHR2. RT-qPCR analysis indicated that the expression levels of *OsRBOH-D* and *OsRBOH-H* were induced in the OsPHR2 overexpression line and suppressed in the *phr2* mutant (Fig. 7a). Promoter analysis indicated that there exists 1 tandem P1BS cis-element (GGA-TATACAGGATATAC) in *OsRBOH-D* promoter (Fig. 7b), implying that *OsRBOH-D* might be a direct target gene of OsPHR2. Dual-LUC reporter assay showed that OsPHR2 promoted the LUC activity driven by *OsRBOH-D* promoter, which was enhanced upon LP or H₂O₂ treatment (Fig. 7c, d). The LUC activity was not significantly affected in the C140 mutation, and in contrast, it was significantly decreased in the C377 mutation, which was not responsive to LP or H₂O₂ treatment (Fig. 7d).
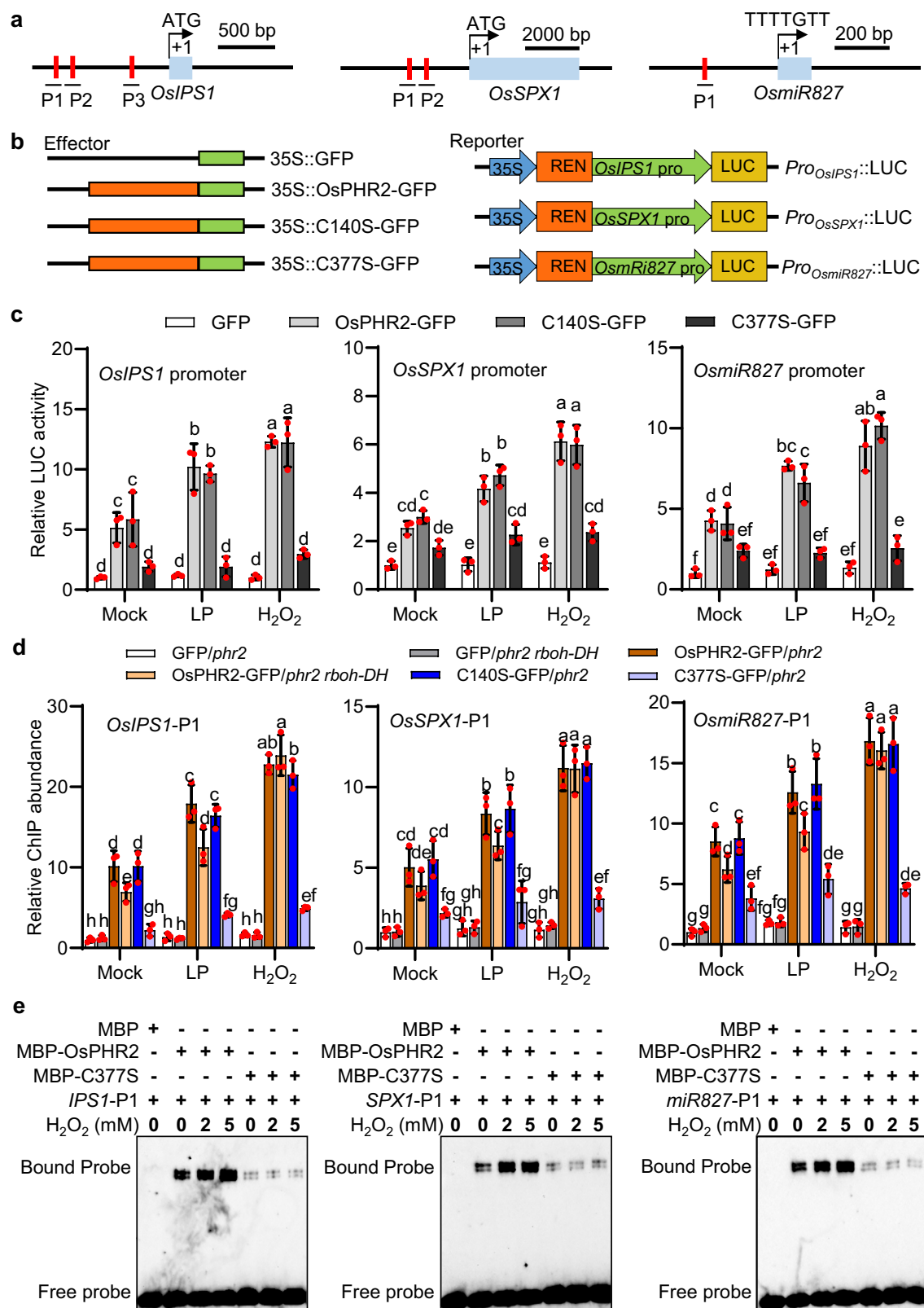
ChIP experiments further confirmed that OsPHR2 directly binds to the *OsRBOH-D* promoter. Moreover, LP-triggered increase of OsPHR2 binding to the *OsRBOH-D* promoter was largely compromised in OsPHR2-GFP/*phr2 rboh-DH* plants, whereas in these plants, the H_2O_2-triggered increase of OsPHR2 binding to the *OsRBOH-D* promoter was essentially unaffected. However, both H_2O_2- and LP-promoted enrichment of OsPHR2 binding to the *OsRBOH-D* promoter were

largely abolished with the C377S mutation but not with the C140S mutation on OsPHR2 (Fig. 7e).

In vitro EMSA experiments showed that OsPHR2 bound to the *OsRBOH-D* promoter (Fig. 7f), which was largely attenuated by adding the unlabeled competitor or competitor mutated in the flanking sequence of P1BS motif, but not by a competitor mutated in the P1BS motif (Fig. 7f, g). In addition, H_2O_2-treated OsPHR2 displayed greater

Fig. 5 | LP-induced H_2O_2 enhances OsPHR2 binding affinity to target promoters. **a** The schematic diagram of the *OsIPS1*, *OsSPX1*, and *OsmiR827* genomic region. P1, P2, or P3 of the indicated genes represents the DNA fragments for the ChIP-qPCR assays. Red short lines indicate the positions of the P1BS motif. **b, c** Dual-luciferase (LUC) reporter gene assays of transcription activation of OsPHR2 and its mutated variants on the promoter of *OsIPS1*, *OsSPX1*, and *OsmiR827* in leaves of *N. benthamiana* plants treated with 2 mM H_2O_2 or LP. GFP, OsPHR2-GFP, C140S-GFP, or C377S-GFP was used as effector, and LUC driven by *OsIPS1*, *OsSPX1*, or *OsmiR827* promoter was used as reporter. The activity of *OsIPS1*::LUC + GFP, *OsSPX1*::LUC + GFP, or *OsmiR827*::LUC + GFP under mock conditions was set to 1. **d** Enrichment of the indicated DNA fragments in ChIP-qPCR assays. Chromatin from GFP/*phr2*, GFP/*phr2rboh-DH*, OsPHR2-GFP/*phr2*, OsPHR2-GFP/*phr2rboh-DH*, C140S-GFP/*phr2* and C377S-GFP/*phr2* plants treated with 2 mM H_2O_2 or LP for an additional 2 days were immunoprecipitated using the anti-GFP antibody and then used for qPCR. For each probe, the expression level in different plants was normalized to GFP/*phr2* plants under mock conditions (which was set as 1). **e** The effects of H_2O_2 on the binding affinity of MBP-OsPHR2 or MBP-C377S to the indicated probes determined by EMSA assay. The EMSA analysis was repeated three times with similar results for (**e**). Data are means ± SD (n = 3 replicates for **c** and **d**). The different letters above the bars denote significant differences ($P < 0.05$) according to a two-sided Duncan's multiple range test. Source data are provided in the Source Data file.

binding ability than the untreated protein to the *OsRBOH-D* probe, while mutation of OsPHR2 at Cys377 dramatically disrupted its binding ability to the probe in either presence or absence of H_2O_2 (Fig. 7f). These findings indicate that H_2O_2-mediated oxidation of OsPHR2 Cys377 enhances its binding ability to the *OsRBOH-D* promoter. All the above results indicate that *OsRBOH-D* is a direct target gene of OsPHR2 and that Cys377 plays an essential role on LP- or H_2O_2-induced OsPHR2 binding ability to the *OsRBOH-D* promoter.

Discussion
H_2O_2 is a key intracellular signaling molecule in the response to different stresses, such as drought, heat, and cold stress[34–38]. This study extends on this key role of H_2O_2 by showing that it is also involved in the control of Pi starvation responses to promote LP adaptation, and uncovers the underlying mechanism. Specifically, we demonstrated that LP-induced H_2O_2 production is mediated by OsRBOH-D/H, causing the oxidation of OsPHR2 at Cys377, which in turn facilitates its oligomerization and enhances its nuclear translocation and DNA-binding ability. As a consequence, there is an increased activation of PSI genes, including *OsRBOH-D/H* and concomitantly of Pi starvation responses (Fig. 7h). These findings add a new regulatory layer to the ones already established in the control of OsPHR2, that include the negative control by SPX sensors, HRZ1/2-mediated ubiquitination to promote its degradation and GSK2-mediated phosphorylation to inhibit its DNA-binding ability[19,20,22,26].

Compared with the about 5 day delayed transcriptome reprogramming, morphological remodeling, or Pi remobilization and redistribution of the typical Pi-starvation responses reported in previous studies[11–15,57], our results showed that both H_2O_2 accumulation and the expression of *OsRBOH-D/H* and PSI genes are detectable as early as 1 day after LP treatment (Supplementary Fig. 1a and Supplementary Fig. 15), which means that LP-induced H_2O_2 might regulate PSI gene expression and LP adaptation after 1 day phosphate deficiency. While H_2O_2 levels and *OsRBOH-D/H* expression peaked by day 4, PSI gene expression continues to rise beyond 7 days (Supplementary Fig. 15). This suggests that H_2O_2 serves as an early signal that accelerates the initial activation of PSI genes, with later expression being at least in part independent of H_2O_2. The observation that OsPHR2 activates *OsRBOH-D/H* expression and that OsRBOH-D/H in turn promotes OsPHR2 activity reveals a positive feedback loop. This loop enhances H_2O_2 production, which further activates OsPHR2, thereby amplifying the transcriptional response during the early phase of Pi starvation. Supporting this model, exogenous H_2O_2 enhances Pi starvation responses, whereas chemical scavenging of H_2O_2 or genetic disruption of *OsRBOH-D/H* impairs OsPHR2-mediated responses, including PSI gene expression and Pi acquisition under LP conditions (Fig. 1), indicating that H_2O_2 is indeed critical for proper OsPHR2-mediated activation of Pi-starvation responses. Previous work in *Arabidopsis* identified a local Pi signaling pathway involving ROS production in the root apoplast through malate-mediated Fe accumulation[58–60]. However, this pathway does not account for the ROS effects described here, which are largely mediated by *OsRBOH-D/H*, as indicated by the

impairment of the increase of H_2O_2 accumulation by phosphate starvation in the *rboh-DH* mutant. Moreover, the expression levels of the rice homologous genes of *Arabidopsis LPR1*, *PDR2*, *STOP1* (*SENSITIVE TO PROTON RHIZOTOXICITY*) and *ALMT1* (*ALUMINUM ACTIVATED MALATE TRANSPORTER 1*) were not changed significantly in shoot or root during the early stage under LP treatment (Supplementary Fig. 16).

Although excessive H_2O_2 can be toxic[61], our data indicate that rice mitigates this risk via increased antioxidant enzyme activity at later stages of Pi starvation. Endogenous H_2O_2 levels declined after day 4 of Pi-starvation, which is in line with the increase of CAT and POD activity (Supplementary Fig. 17), the expression upregulation of *CataseA*, *CataseB* and *CataseC* under Pi deficiency after 2 days of Pi-deficiency (Supplementary Fig. 18) and previous reports that the expression level of genes encoding catalase, peroxidase, or superoxide dismutase were up-regulated after 7 days of Pi-starvation responses[57]. These results suggest that rice possesses regulatory mechanisms to scavenge excessive endogenous H_2O_2, ensuring that the OsPHR2-OsRBOH module enhances early signaling without compromising plant performance under Pi deficiency.

We demonstrate that H_2O_2 triggers oxidation of OsPHR2 at Cys377 promotes OsPHR2 oligomerization, nuclear translocation, and also enhances its DNA-binding ability to adapt to a Pi-deficient environment (Fig. 7h). Cys377 is located within the coiled-coil dimerization domain of OsPHR2. Since MYB-CC proteins bind DNA as oligomers[62–64], it is likely that the impaired oligomerization of the OsPHR2C377S underlies its reduced nuclear localization and DNA binding affinity. In line with this, previous studies have shown that mutations in the CC domain of PHR proteins compromise oligomerization and DNA-binding ability in both *Arabidopsis* and rice[62–64]. One plausible explanation for the finding that the C377S mutation impaired its nuclear localization is that OsPHR2 oligomerization, which is impaired in C377S, would prevent its cytoplasmic retention. In agreement with this possibility, it was previously shown that OsPHR2 interacts with OsSPX4, leading to cytoplasmic retention of OsPHR2[19], and our firefly luciferase complementation imaging assay showed that the interaction between OsPHR2 and OsSPX4 is increased by the C377S mutation, but not by mutation at other Cys residues in OsPHR2, and is reduced by LP and H_2O_2 treatments (Supplementary Fig. 19).

Our results further show that H_2O_2 triggers intermolecular disulfide bond formation between OsPHR2 monomers (Fig. 6). The observation that only the mutation of Cys377, but not other cysteine residues in OsPHR2, affects disulfide bond formation (Fig. 6 and Supplementary Fig. 14) strongly suggests that the disulfide bond is established between Cys377 residues from different monomers. OsPHR2 is found in solution as both a dimer and a tetramer[63,64]. The possibility of disulfide bond formation between Cys377 residues within an OsPHR2 dimer is unlikely, because it was found that the two-stranded alpha-helical coils of the AtPHR1 dimer, the OsPHR2 homolog from Arabidopsis, are antiparallel[62]. Consistent with this, our modeling using AlphaFold 3 of the CC domain of OsPHR2 also predicts a similar arrangement for the coiled-coil dimer (Supplementary Fig. 20a). In
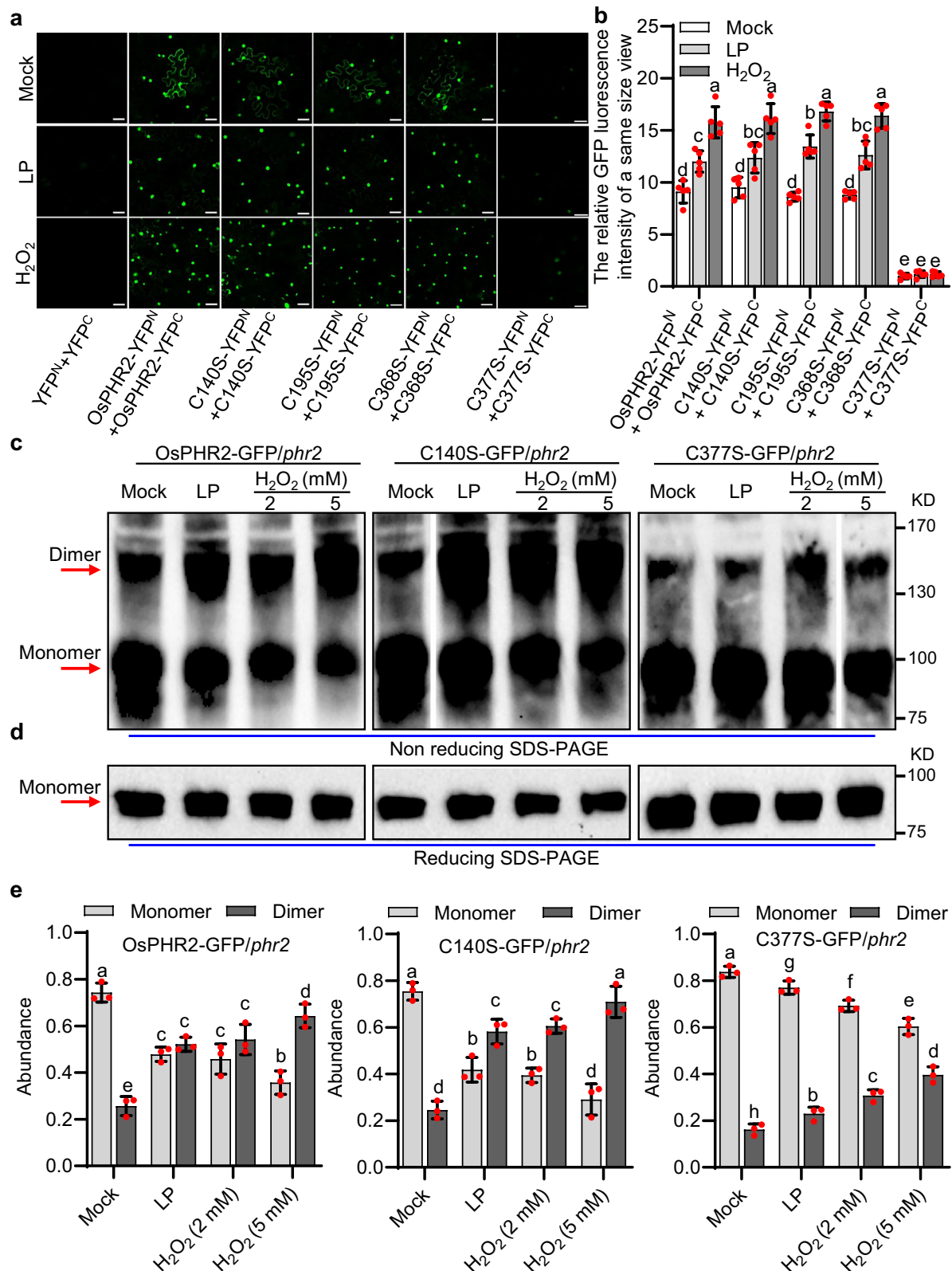
contrast, modeling of the CC domain of OsPHR2 as a tetramer supports disulfide bond formation between Cys377 residues from monomers of its two different dimers (Supplementary Fig. 20b), with the energy of the tetrameric structure with the disulfide bonds similar to that of the optimal structure predicted without disulfide bonds ($-34{,}000$ kJ vs $-35{,}000$ kJ). This model is consistent with the H_2O_2-induced increase in dimer levels observed in wild-type OsPHR2, but

not in OsPHR2-C377S, in non-reducing SDS-PAGE (Fig. 6c and Supplementary Fig. 14), suggesting that disulfide bonds stabilize OsPHR2 tetramers, as the two disulfide bonds in each tetramer are expected to hold together two OsPHR2 dimers. Supporting this notion, the C377S mutant displays reduced oligomer stability, as shown by *in planta* BiFC assays as well as the yeast two hybrid assays (Fig. 6a, b and Supplementary Fig. 13). Of course, the possibility could not be excluded that

Fig. 6 | LP-induced H_2O_2 triggers OsPHR2 oligomerization in plants. a BiFC assay to examine the self-interaction of OsPHR2 and its mutated variants. OsPHR2, C140S, C195S, C368S, and C377S fused with the N-terminal or C-terminal fragments of YFP, respectively, were transiently expressed in leaves of *N. benthamiana* pretreated with 2 mM H_2O_2 or LP for 2 days. After 2 days cultured in darkness, the YFP fluorescence signal was detected using confocal laser scanning microscopy. Bar = 50 μm. **b** The relative fluorescence intensity in a same size view of corresponding samples indicated in (**a**). The reconstituted YFP fluorescence of C377S-YFPN and C377S-YFPC under mock conditions was set to 1. **c**, **d** The effects of H_2O_2 or LP on OsPHR2 oligomerization determined by western blot assays in rice. Total proteins

of 7-day-old 35S::OsPHR2-GFP/*phr2*, 35S::C140S-GFP/*phr2*, and 35S::C377S-GFP/*phr2* plants treated with 2 mM H_2O_2 or LP for an additional 2 days were extracted by cold Native Protein Extraction Buffer (50 mM Tris, pH7.4, 10% glycerol) and separated in Non-reducing SDS-PAGE gels (**c**), or reducing SDS-PAGE gels (**d**), respectively. **e** The relative quantification of monomers and dimers of OsPHR2 in non-reducing SDS-PAGE indicated in (**c**). The immunoblot analysis was repeated three times with similar results for **c** and **d**. Data are means ± SD (*n* = 5 replicates for **b**; *n* = 3 replicates for **e**). The different letters above the bars denote significant differences (*P* < 0.05) according to a two-sided Duncan's multiple range test. Source data are provided in the Source Data file.

the C377-mediated OsPHR2 oligomerization involves changes of protein structure, because the formation of intermolecular disulfide bond often affects the conformation of proteins. In MYC2, tetramerization has been shown to allow this transcription factor to interact with two different DNA binding sites simultaneously, enhancing DNA binding affinity through cooperative interactions of the DNA binding domains with their target sequences[65]. Determining the structure of OsPHR2 bound to DNA will clarify whether its tetramerization has a similar functional impact.

Interestingly, among the 11 OsPHR2 homologs in rice[66], OsPHR1, OsPHR9, or OsPHR10 shares the Cys residue at the corresponding site with OsPHR2 Cys377, and a BLAST search in the Phytozome database[67] revealed that the predominant residue at the equivalent position of Cys377 in OsPHR2 is not Cys, but Gln (Q), in its homologs in plants (Supplementary Table 1), suggesting Q is the ancestral residue. In fact, this Q is present in at least one OsPHR2 homolog across a wide range of plant species from various taxonomic groups, including the liverwort *Marchantia polymorpha*, the fern *Ceratopteris richardii*, and numerous gymnosperms and angiosperms, both monocots and dicots. Notable exceptions to this pattern include *Solanum lycopersicum* (see Supplementary Table 1). The presence of PHR2 homologs with a Cys residue at the equivalent position of Cys 377 of OsPHR2 appears to be restricted to gymnosperms and angiosperms, in which there are also species lacking it (e.g., *Ginkgo biloba* and *Solanum lycopersicum*). This raises the intriguing possibility that H_2O_2 regulation via Cys377-mediated OsPHR2 oligomerization may be a more recent evolutionary adaptation. Future studies should investigate whether H_2O_2 functions similarly in Pi signaling across plant species lacking a Cys377-containing MYB-CC protein.

Methods
Plant materials and growth conditions
All rice (*Oryza sativa*) plants used in this study were derived from the *japonica* variety Xiushui 134 (XS134). The plants expressing OsPHR2-mCherry, OsPHR2-GFP, C140S-GFP, C195S-GFP, C368S-GFP or C377S-GFP fusion proteins were obtained by transforming 35S::OsPHR2-mCherry, 35S::OsPHR2-GFP, 35S::C140S-GFP, 35S::C195S-GFP, 35S::C368S-GFP or 35S::C377S-GFP into XS134, respectively. The single mutant *rboh-D*, *rboh-H*, *phr2* and double mutant *rboh-DH* in the XS134 background were generated using the CRISPR/Cas9 technique as previously described[68]; the plants expressing OsPHR2-mCherry fusion proteins in *rboh-DH* background were obtained by transforming 35S::OsPHR2-mCherry into *rboh-DH* mutant background; the plants expressing OsPHR2-GFP, C140S-GFP, C195S-GFP, C368S-GFP, or C377S-GFP fusion proteins in *phr2* mutant background was obtained by transforming 35S::OsPHR2-GFP, 35S::C140S-GFP, 35S::C195S-GFP, 35S::C368S-GFP or 35S::C377S-GFP into *phr2* mutant, respectively. Rice or *Nicotiana benthamiana* plants were grown under natural conditions or on modified hydroponic solution ($MgSO_4·7H_2O$ 547 μM, $(NH_4)_2SO_4$ 365 μM, KH_2PO_4 200 μM, KNO_3 183 μM, $Ca(NO_3)_2·4H_2O$ 366 μM, $MnCl_2·4H_2O$ 0.5 μM, H_3BO_3 3 μM, $(NH_4)_6Mo_7O_{24}·4H_2O$ 0.1 μM, $ZnSO_4·7H_2O$ 0.4 μM, $CuSO_4·5H_2O$ 0.2 μM, NaFe(3)-EDTA·$3H_2O$ 40 μM) in a growth chamber. The hydroponic solution was adjusted to pH 5.5

with KOH and replaced every 3 days. Experiments were carried out in a growth chamber with a 12 h day (30 °C)/12 h night (22 °C) photoperiod, with a 200 μmol m^{-2} s^{-1} photon density and 60% humidity.

H_2O_2, KI, or LP treatment
For examining H_2O_2 content, 7-day-old rice plants were cultured hydroponically under high Pi (HP; 200 μM KH_2PO_4) or low Pi (LP; 10 μM KH_2PO_4) conditions for the indicated days, the shoot and root tissues of those plants were obtained and used for examinations. For examining gene expression in response to exogenous H_2O_2 or KI treatment in time course assay, 7-day-old rice plants were treated hydroponically with 10 mM H_2O_2 or 1 mM KI added directly into the nutrient solution for indicated times, the shoots and roots of those plants were obtained and used for examinations. For examining gene expression in response to LP treatment, 7-day-old rice plants were treated hydroponically under HP or LP conditions for the indicated days, and then the shoots and roots of those plants were obtained and used for examinations. For examining Pi concentrations, 7-day-old rice plants were treated hydroponically under HP or LP conditions for an additional 5 days, and then the shoots and roots of those plants were sampled for examination. For phenotypic analysis under H_2O_2 or KI treatments, rice seeds were sowed in nylon mesh after germination and treated hydroponically for 28 days under HP or LP conditions with different concentrations of H_2O_2 (1 mM, 2 mM, 3 mM, 4 mM, and 5 mM) or KI (1 μM, 10 μM and 100 μM) in the nutrient solution, then the shoots and roots of those plants were obtained to examine biomass (dry weight).

Vector construction and plant transformation
To generate 35S::OsPHR2-mCherry or 35S::OsPHR2-GFP vector, the entire coding sequences (CDSs) of OsPHR2 (Os07g0438800) was amplified from 'XS134' cDNA using PCR with Phanta HS Super-Fidelity DNA Polymerase (Vazyme, Cat: P502-d1) and cloned into the modified binary expression vector pCAMBIA1300-mCherry under the control of cauliflower mosaic virus 35S promoter at the *Sac*I and *Bam*HI sites or cloned into a modified binary expression vector pCAMBIA1300-GFP under the control of cauliflower mosaic virus 35S promoter at the *Sac*I and *Bam*HI sites with ClonExpress II One Step Cloning Kit (Vazyme, Cat: C112-02). To generate the mutated variants 35S::C140S-GFP, 35S::C195S-GFP, 35S::C368S-GFP, and 35S::C377S-GFP vectors, the overlap PCR-mediated site-directed mutagenesis was performed to generate the corresponding variant, and then cloned into a modified binary expression vector pCAMBIA1300-GFP under the control of 35S promoter at the *Sac*I and *Bam*HI sites with ClonExpress II One Step Cloning Kit. The vectors CRISPR-OsPHR2, CRISPR-RBOH-D (Os05g0465800), CRISPR-RBOH-H (Os12g0541300) and CRISPR-RBOH-D/RBOH-H were designed and constructed according to the instructions described previously[68]. After confirmed by sequencing, the resultant constructs were transformed into callus induced from mature embryos of the corresponding rice materials via *Agrobacterium tumefaciens* (strain EHA105) mediated transformation as described previously[69]. The primers used for the generation of these constructs are listed in Supplementary Table 2.
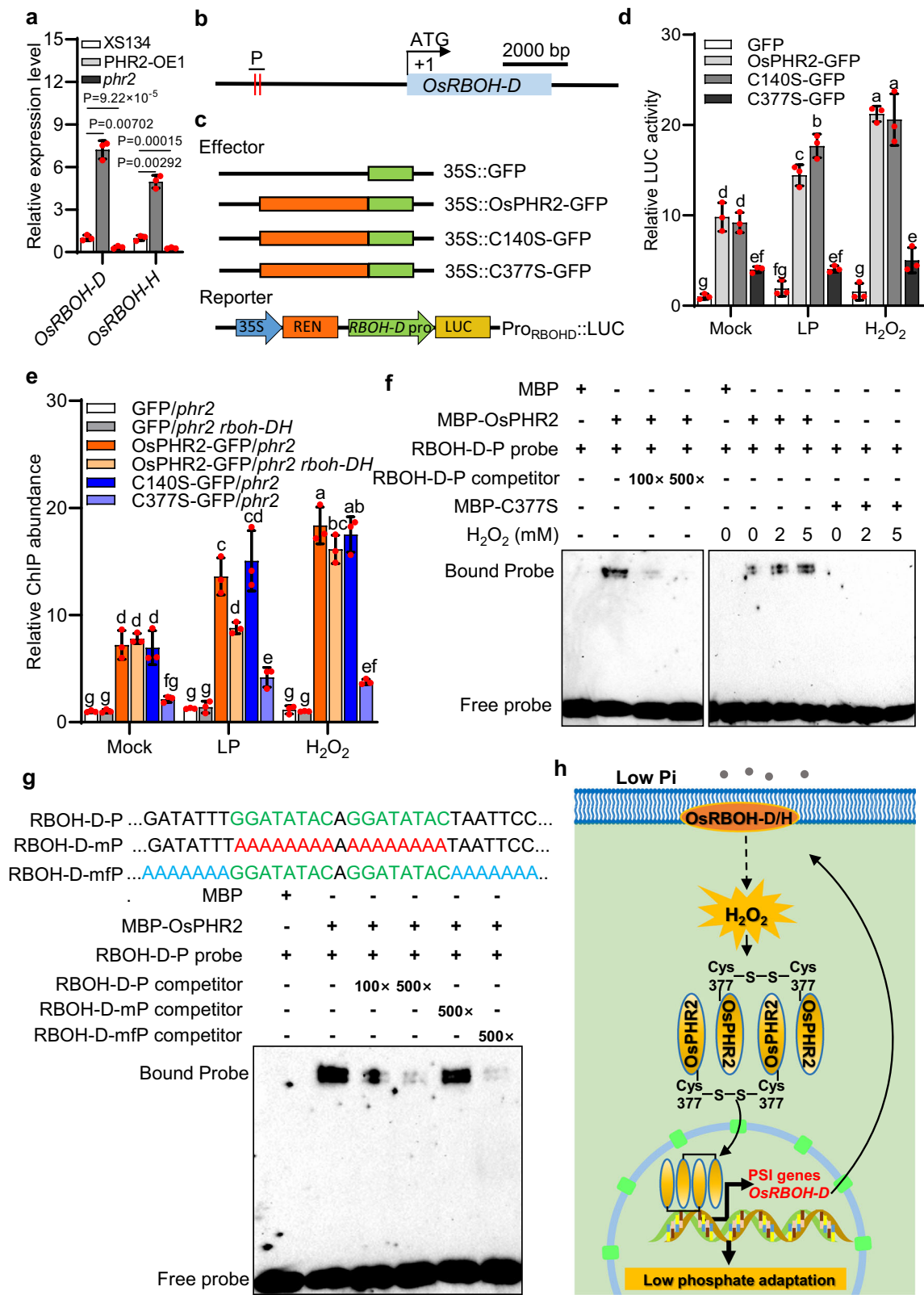
RNA isolation, reverse transcription polymerase chain reaction (RT-PCR), and reverse transcription quantitative real-time PCR (RT-qPCR) assays

Plant tissues were harvested and ground in liquid nitrogen, and total RNA was extracted using TRIzol reagent (Life Technologies) according to the manufacturer's protocol. The first strand cDNA synthesis was obtained by HiScript II 1st Strand cDNA Synthesis Kit (Vazyme, Cat: R211-01) for gene clone, or by HiScript II QRT SuperMix for qPCR (+ gDNA wiper) (Vazyme, Cat: R223-01) for RT-qPCR, following the protocol. For RT-qPCR, the cDNA samples were diluted and triplicate quantitative assays were performed with 2 μL of each cDNA dilution and 3 μL primers with the ChamQ Blue Universal SYBR qPCR Master Mix (Vazyme, Q312-02). The relative quantification method (-ΔΔCT) was used to normalize quantitative variation between the replicates.

Fig. 7 | OsRBOH-D is a direct target gene of OsPHR2. a The relative expression levels of *OsRBOH-D* and *OsRBOH-H* in wild type XS134, *OsPHR2* overexpression plant (PHR2-OE1) and *phr2* mutant determined by RT-qPCR. *OsACTIN1* was used as an internal control. **b** A schematic diagram of the *OsRBOH-D* genomic region. P represents the DNA fragments amplified in the ChIP-qPCR assays. Red short lines indicate the positions of the P1BS motif. **c**, **d** Dual-luciferase (LUC) reporter gene assays to examine the role of OsPHR2 on *OsRBOH-D* expression in leaves of *N. benthamiana* plants pretreated with 2 mM H_2O_2 or LP for 2 days. GFP, OsPHR2-GFP, C140S-GFP, or C377S-GFP were used as an effector, and LUC driven by the *OsRBOH-D* promoter was used as a reporter. The LUC activity of *OsRBOH-Dpro*::LUC + GFP under mock conditions was set to 1. **e** Enrichment of the *OsRBOH-D* promoter fragment indicated in ChIP assays. Chromatin from 7-day-old GFP/*phr2*, GFP/*phr2rboh-DH*, OsPHR2-GFP/*phr2*, OsPHR2-GFP/*phr2rboh-DH*, C140S-GFP/*phr2*, and C377S-GFP/*phr2* plants treated with 2 mM H_2O_2 or LP for an additional 2 days were immunoprecipitated using the anti-GFP antibody and then used for qPCR. **f** The binding affinity of MBP-OsPHR2 to *OsRBOH-D* promoter (left) and the effects of H_2O_2 on the binding affinity of MBP-OsPHR2 or MBP-C377S to *OsRBOH-D* promoter (right) determined by EMSA assay. **g** Mutations in the binding motif of *OsRBOH-D* promoter (RBOH-D-mP) reduce the binding intensity of OsPHR2 to the *OsRBOH-D* promoter determined by EMSA assay. **h** Working model for the mechanism underlying LP-triggered H_2O_2 accumulation and its effect on OsPHR2 to enhance Pi-starvation responses in rice. Under LP stress, *OsRBOH-D/H* are rapidly induced to facilitate H_2O_2 production to oxidize OsPHR2 at Cys377, which promotes the Cys377/Cys777-mediated oligomerization of OsPHR2 to enhance its nuclear translocation and DNA binding ability to promoters of PSI genes, including *OsRBOH-D*, thus activating their expression to improve rice LP adaptation. The EMSA analysis was repeated three times with similar results for **f** and **g**. Data are means ± SD (*n* = 3 replicates for **a**, **d**, and **e**). The *P*-value was generated from a two-sided Student's *t* test for a. Different letters above the bars denote significant differences (*P* < 0.05) according to a two-sided Duncan's multiple range test for **d** and **e**. Source data are provided in the Source Data file.

The rice *OsACTIN1* gene was used as an internal control. Three replicates were performed for each gene.

H_2O_2 measurement

The H_2O_2 levels were examined as described previously[70]. Briefly, freshly harvested materials were ground into powder in liquid nitrogen, and then added 1 M $HClO_4$ containing 5% PVP. Once thawed, centrifuge at 4 °C and 14 000 r.p.m. for 10 min. Add 100 μL of 0.2 M phosphate buffer (pH 5.6) to an aliquot of 0.5 mL of the supernatant and adjust to pH 5 using 3 M K_2CO_3. Then centrifuge for 30 s to remove insoluble $KClO_4$. Incubate 50 μL of the neutralized extract for 10 min with 1 unit of ascorbate oxidase (AO) to oxidize ascorbate. Add 870 μL 0.1 M phosphate buffer (pH 6.5), 20 μL freshly prepared 165 mM 3-(dimethylamino) benzoic acid (DMAB), 50 μL freshly prepared 1.4 mM 3-methyl-2-benzothiazoline hydazone (MBTH) and 50 ng of peroxidase to the cuvette. Initiate the reaction by adding 50 μL of the extract. Monitor changes in A590 at 25 °C. Prepare and read H_2O_2 standards ranging from 0 to 2 nmol for each experiment. Measure at least in triplicate for each extract or H_2O_2 standards.

POD and CAT activity measurements

The enzymatic activities of POD and CAT were determined as previously described[71] using the Peroxidase Assay Kit (A084-1-1) and the Catalase Assay Kit (A007-1-1; Nanjing Jiancheng Bioengineering Institute, China). The unit of catalase activity is defined as decomposing 1 μmol H_2O_2 per minute per gram sample at 37 °C, and the unit of peroxidase activity is defined as catalyzing 1 μmol substrate per minute per gram sample at 37 °C. Three biological replicates were conducted.

Phosphate (Pi) measurement

Inorganic Pi measurements were performed as described previously[72]. Briefly, the fresh samples were homogenized in 2 mL 1% (v/v) of acetic acid using a lyser (TissueLyserII, QIAGEN, Dusseldorf, Germany) and then placed in 4 °C for 60 min. The homogenate was then diluted and filtered 10 times with H_2O. After filtration, the filtrate was used for Pi measurement via the molybdenum blue method: 0.4% (w/v) ammonium molybdate melted in 0.5 M H_2SO_4 (solution A) was mixed with 10% ascorbic acid (solution B; A:B, 6:1). Two milliliters of this work solution were added to 1 mL of the sample solution, and incubated in a water bath at 37 °C for 60 min. After being cooled on ice, the absorbance was measured at 820 nm wavelength. Pi concentration was calculated by normalizing the fresh weight.

Protein expression and purification

The full-length CDS of OsPHR2, C140S, C195S, C368S, and C377S were cloned into the *Bam*HI and *Pst*I sites of prokaryotic expression vector pMAL-p2X under the control of 35S promoter using ClonExpress II One Step Cloning Kit to generate MBP-OsPHR2, MBP-C140S, MBP-C195S,

MBP-C368S, and MBP-C377S vectors. The resultant plasmids were introduced into E. *coli* BL21 (DE3). The expression and purification of those MBP-fused OsPHR2 and its mutated variants were performed as described previously[35]. The primers used for the generation of these constructs are listed in Supplementary Table 2.

BIAM labeling assay

BIAM labeling assay was conducted according to the previous description[37] with slightly modifications. The MBP and MBP-OsPHR2 proteins treated with different concentrations of H_2O_2 in PBS buffer (NaCl 137 mM, KCl 2.7 mM, Na_2HPO_4 10 mM, KH_2PO_4 2 mM) at room temperature for 30 min. The proteins were precipitated by adding one volume of acetone at − 20 °C for 20 min and centrifuged at 10000 g for 5 min. The pellets were washed three times with 50% acetone and dissolved in labeling buffer (50 mM MES-NaOH, pH 6.5, 100 mM NaCl, 1% TritonX-100, 100 μM BIAM), and then incubated at room temperature in the dark for 2 h. The labeling reactions were terminated by the addition of β-mercaptoethanol to a final concentration of 50 mM. The reaction mixtures were precipitated by adding one volume of acetone at − 20 °C for 30 min and centrifuged at 10000 × *g* for 5 min. The pellets were dissolved in SDS sample buffer and subjected to separate on SDS-PAGE. Proteins labeled with BIAM were detected with HRP-conjugated streptavidin antibody (Thermo Scientific, Cat: N100, 1:2000 dilution). The total MBP or MBP-OsPHR2 proteins were detected by anti-MBP antibody (ABclonal, Cat: AE016, 1:2000 dilution).

In vivo and in vitro biotin-switch assays

Biotin-switch assays were performed as previously described[37] with slight modification. For in vivo oxidation analysis, the 7-day-old transgenic plants were treated with or without 2 mM H_2O_2 or LP for another 2 days and the proteins were extracted with PEB (protein extraction buffer) (50 mM Tris-HCl (pH 8.5), 150 mM NaCl, 1 mM EDTA, 10% glycerol (v/v), 1% SDS (w/v), 1 × Protease Inhibitor Cocktail, 5 mM PMFS). For in vitro oxidation analysis, the MBP-OsPHR2 fusion protein expressed and purified from E. *coli* was treated with 5 mM H_2O_2 or 1 mM DTT at room temperature for 30 min and then precipitated by adding one volume of acetone at − 20 °C for 30 min followed by centrifugation at 10000 × *g* for 5 min. The pellet was washed three times with 50% acetone and dissolved in PEB buffer. To detect the oxidized form of OsPHR2, the plant protein extracts or the recombinant OsPHR2 proteins were incubated with 100 mM NEM in the PEB buffer at room temperature for 30 min with frequent vortexing to block free thiol. The samples were precipitated with one volume of acetone and washed three times with 50% acetone. The pellets were dissolved in PEB buffer plus 20 mM DTT, and then incubated at 37 °C for 30 min to reduce the oxidized thiols. DTT was removed by protein precipitation, and pellets were resuspended in PEB buffer. The supernatant was labeled with 100 μM BIAM at room temperature for 1 h in the dark, and

proteins were precipitated with one volume of acetone to remove free BIAM. The BIAM-treated proteins were then dissolved in PEB buffer and diluted by Wash Buffer (50 mM Tris-HCl (pH 7.5), 100 mM NaCl, 1 mM EDTA, 1 mM PMSF and 1 × protease inhibitor cocktail). After centrifugation at 10,000 × g for 5 min, the supernatant was added to streptavidin beads (Roche, Cat: 11641778001) and incubated at 4 °C for 4 h. Beads were washed five times with Wash Buffer, and proteins were dissolved in 2 × SDS sample buffer, and the samples were separated on 4–20% SDS-PAGE gels. The gel blots were probed with anti-mCherry antibody (Elabscience, Cat: E-AB-48007, 1:2000 dilution), anti-GFP antibody (ABclonal, Cat: AE012, 1:2000 dilution) or anti-MBP antibody (ABclonal, Cat: AE016, 1:2000 dilution).

Subcellular localization assay

To assay the subcellular localization of OsPHR2 and its mutated variants in plants, leaves of 28-day-old *N. benthamiana* plants pretreated with 2 mM H_2O_2 or LP for 2 days were used to express the indicated GFP-fused proteins using *Agrobacterium*-mediated transformation. After 2 days growth in darkness, the GFP fluorescence was observed under a confocal laser scanning microscope (LSM710, Zeiss, Oberkochen, Germany). 7-day-old 35S::OsPHR2-GFP/*phr2*, 35S::OsPHR2C140S/*phr2* and 35S::OsPHR2C377S-GFP/*phr2* transgenic plants were used for the examination of the subcellular localization of OsPHR2, OsPHR2C140S, and OsPHR2C377. The plants were treated with LP or 2 mM H_2O_2 for an additional 2 days, then the GFP fluorescence in roots was observed under a confocal laser scanning microscope (LSM710, Zeiss, Oberkochen, Germany). Finally, the ImageJ software was used for calculating the ratio of nuclear fluorescence intensity/total fluorescence intensity within cells.

The cytoplasmic and nuclear accumulation of OsPHR2 was assayed with immunoblot detection. 7-day-old indicated rice plants were treated with 2 mM H_2O_2 or LP for 2 days, and half of the sample was used to extract total proteins, while the other half was used to extract cytosolic and nuclear proteins, as described previously[41]. As the nuclear fraction was condensed, whereas the soluble fraction was not, the nuclear and soluble samples cannot be directly compared. Histone3 and actin were assayed using the anti-H3 and anti-ACTIN antibodies as loading controls for nuclear and cytoplasmic proteins, respectively.

Dual-luciferase reporter gene assays

The *OsIPS1* promoter, *OsSPX1* promoter, *OsmiR827* promoter, or *OsRBOH-D* promoter was amplified using PCR from 'XS134' DNA with Phanta HS Super-Fidelity DNA Polymerase, then inserted into a pGreenII 0800-LUC vector[73] at the *Kpn*I and *BamH*I sites with ClonExpress II One Step Cloning Kit to generate IPS1p::LUC, SPX1p::LUC, miR827p::LUC, and RBOH-Dp::LUC, respectively. The resultant plasmids were co-expressed with GFP, OsPHR2-GFP, C140S-GFP, and C377S-GFP in leaves of 28-day-old *N. benthamiana* plants pretreated with 2 mM H_2O_2 or LP for 2 days by *Agrobacterium*-mediated transformation. After 2 days growth in darkness, the firefly LUC and Renilla luciferase (REN) activities were detected. The LUC/REN ratio represents the activity relative to the internal control (REN driven by the 35S promoter). The primers used for the generation of these constructs are listed in Supplementary Table 2.

Chromatin immunoprecipitation (ChIP) qRT-PCR assay

The ChIP-qPCR was performed as previously described[74] with slightly modified, 7-day-old 35S::GFP/*phr2*, 35S::GFP/*phr2 rboh-DH*, 35S::OsPHR2-GFP/*phr2*, 35S::OsPHR2-GFP/*phr2 rboh-DH*, 35S::C140S-GFP/*phr2*, and 35S::C377S-GFP/*phr2* transgenic rice plants were treated with 2 mM H_2O_2 or LP for 2 days and then fixed in 1% formaldehyde for 15 min at room temperature under a vacuum. Fixed tissues were ground into fine powder in liquid nitrogen, and the nuclei were isolated. The chromatin released from the nuclei was sonicated into 200–500 bp fragments.

One-half was used as an input, with the remaining half used for immunoprecipitation with anti-GFP antibody (ABclonal, Cat: AE012, 1:2000 dilution). The immunoprecipitated DNA fragments were used to perform RT-qPCR assays. The primers used for the ChIP qPCR assay are listed in Supplementary Table 2.

Electrophoretic mobility shift assay (EMSA)

The EMSA assay was performed as described[41], oligonucleotide probes for the EMSA assay were first labeled with biotin at their 3'-ends using a Biotin 3' End DNA labeling Kit (Thermo Fisher Scientific). The EMSA assay was performed using a Light Shift Chemiluminescent EMSA kit (Thermo Fisher Scientific), according to the manufacturer's instructions. Specifically, for H_2O_2 treatments, different concentrations of H_2O_2 (0, 2 and 5 mM) were used to treat the proteins for 30 min. The probe sequences used for the EMSA assay are listed in Supplementary Table 2.

Yeast two hybrid (Y2H) assay

The matchmaker GAL4 two-hybrid system (Clontech) was used for Y2H assays. The coding sequences (CDSs) of OsPHR2 and its mutated variants were cloned into the pGADT7 vector with *Nde*I and *Pst*I or the pGBKT7 vector with *Nde*I and *BamH*I, respectively, to generate AD-OsPHR2, AD-C140S, AD-C195S, AD-C368S, AD-C377S and BD-OsPHR2, BD-C140S, BD-C195S, BD-C368S, BD-C377S vectors. The β-galactosidase liquid assays were performed as previously described[75]. Different vector combinations were cotransformed into yeast (AH109). The selection medium used was SD/-W-L (without tryptophan and leucine, for selecting positive clones), SD/-W-L-H (without tryptophan, leucine, and histidine, for selecting positive interaction clones) and SD/-W-L-H-A (without tryptophan, leucine, histidine, and adenine, for selecting positive interaction clones). The primers used for the Y2H assay are listed in Supplementary Table 2.

Bimolecular fluorescence complementation (BiFC) assay

The BiFC assay was performed as described[41] with slightly modified. The coding sequences (CDSs) of OsPHR2 and its mutated variants were cloned into the p2YFN (containing the N-terminal sequence of YFP) vector and p2YFC vector (containing the C-terminal sequence of YFP) with *Pac*I and *Sgs*I, respectively, to generate p2YFN-OsPHR2, p2YFN-C140S, p2YFN-C195S, p2YFN-C368S, p2YFN-C377S and p2YFC-OsPHR2, p2YFC-C140S, p2YFC-C195S, p2YFC-C368S, p2YFC-C377S. The resultant plasmids were introduced into *Agrobacterium* (EHA105), which were used to infiltrate *N. benthamiana* leaves of *N. benthamiana* plants pretreated with 2 mM H_2O_2 or LP for 2 days. After 2 days growth in darkness, the reconstituted YFP fluorescent signal (500 nm excitation/542 nm emission) was detected using a confocal laser scanning microscope (LSM710, Zeiss, Oberkochen, Germany). The primers used for the BiFC assay are listed in Supplementary Table 2.

OsPHR2 oligomerization assay

To assay the oligomerization of OsPHR2 and its mutated variants in vivo, 7-day-old 35S::OsPHR2-GFP/*phr2*, 35S::C140S-GFP/*phr2*, 35S::C195S-GFP/*phr2*, 35S::C368S-GFP/*phr2*, and 35S::C377S-GFP/*phr2* transgenic rice plants were ground into fine powder in liquid nitrogen, and then added cold protein extraction buffer (50 mM Tris, pH7.4, 10% glycerol). After centrifugation at 12000 × g for 10 min at 4 °C, total soluble proteins were carefully extracted and then treated with or without 50 mM DTT for 4 h at room temperature. After treatment, the samples were separated in non-reducing SDS-PAGE gels or reducing SDS-PAGE gels, respectively. To examine H_2O_2- or LP-induced OsPHR2 oligomerization in vivo, 7-day-old 35S::OsPHR2-GFP/*phr2*, 35S::C140S-GFP/*phr2*, and 35S::C377S-GFP/*phr2* transgenic plants were treated with indicated H_2O_2 concentrations or LP for 2 days. The OsPHR2-GFP proteins in different gels were immunoblotted with the anti-GFP antibody (ABclonal, Cat: AE012, 1:2000 dilution), respectively.

Luciferase Complementation Imaging (LCI) assay

The coding sequences of OsSPX4 and OsPHR2 or its mutated variants were amplified using PCR from 'XS134' cDNA with Phanta HS Super-Fidelity DNA Polymerase, then inserted into a pCAMBIA1300-cLUC and pCAMBIA1300-nLUC vector at the *SacI* and *SalI* sites with ClonExpress II One Step Cloning Kit to generate OsSPX4-cLUC, OsPHR2-nLUC, C140S-nLUC, C195S-nLUC, C368S-nLUC and C377S-nLUC, respectively. The resultant plasmids were co-expressed in leaves of 28-day-old *N. benthamiana* plants pretreated with 2 mM H_2O_2 or LP for 2 days by *Agrobacterium*-mediated transformation with four different construct combinations: OsPHR2-nLUC and OsSPX4-cLUC, C140S-nLUC and OsSPX4-cLUC, C195S-nLUC and OsSPX4-cLUC, C368S-nLUC and OsSPX4-cLUC, C377S-nLUC and OsSPX4-cLUC. After 2 days growth in darkness, images of luminescence were captured using a low-light-cooled CCD imaging apparatus (NightSHADE LB985, Berthold Technologies GmbH & Co.KG, Germany). Representative images of at least five tobacco leaves were presented. The primers used for generating these constructs are listed in Supplementary Table 2.

Bioinformatics and computer modeling

To examine Cys377 conservation in plant MYB-CC proteins, Blast searches in the PHYTOZOME database[67] were conducted in the species indicated in Supplementary Table 1 using the consensus sequence of the CC domain between OsPHR2 and its functional homolog in *Arabidopsis* AtPHR1 (consensus sequence: TEALRL QXEXQKXLHE QLEIQRXLQLRIEEQGKXLQ MMXEXQ)

The amino acid sequence of OsPHR2 encompassing its coiled-coil region was used to build models of the dimer and tetramer using AlphaFold 3[76]. The resulting models were visualized using UCSF Chimera[77] and subjected to structural refinement either with or without the disulfide bond in Cys 377.

Statistical analysis

Unless specific explanation, all data were analyzed using SPSS statistical software (SPSS 17.0, IBM). The statistical significance among multiple datasets was determined using a two-side Duncan's multiple range test; the statistical significance between two groups was determined using two-sided Student's *t* test.

Reporting summary

Further information on research design is available in the Nature Portfolio Reporting Summary linked to this article.

Data availability

The sequence of genes used in this study can be found in the Rice Annotation Project (RAP) (https://rapdb.dna.affrc.go.jp/index.html) under related accession number: *OsPHR2/Os07g0438800*; *OsACTIN1/Os03g0718100*; *OsIPS1/Os03g0146800*; *OsSPX1/Os06g0603600*; *OsPT10/Os06g0325200*; *OsRBOH-A/Os01g0734200*; *OsRBOH-B/Os01g0360200*; *OsRBOH-C/Os05g0528000*; *OsRBOH-D/Os05g0465800*; *OsRBOH-E/Os01g0835500*; *OsRBOH-F/Os08g0453700*; *OsRBOH-G/Os09g0438000*; *OsRBOH-H/Os12g0541300*; *OsRBOH-I/Os11g0537400*; *OsCataseA/Os02g0115700*; *OsCataseB/Os06g0727200*; *OsCataseC/Os03g0131200*; *OsART1/Os12g0170400*; *OsLPR1/Os01g0126100*; *OsALMT1/Os04g0417000*; *OsPDR2/Os05g0402800*. Source data are provided in this paper.

References

1. Jia, X., Wang, L., Nussaume, L. & Yi, K. Cracking the code of plant central phosphate signaling. *Trends Plant Sci.* **28**, 267–270 (2022).
2. Vance, C. P., Uhde-Stone, C. & Allan, D. L. Phosphorus acquisition and use: critical adaptations by plants for securing a nonrenewable resource. *N. Phytol.* **157**, 423–447 (2003).
3. Lu, H. et al. Molecular mechanisms and genetic improvement of low-phosphorus tolerance in rice. *Plant Cell Environ.* **46**, 1104–1119 (2024).
4. Paz-Ares, J. et al. Plant adaptation to low phosphorus availability: core signaling, crosstalks, and applied implications. *Mol. Plant* **15**, 104–124 (2022).
5. Foley, J. A. et al. Solutions for a cultivated planet. *Nature* **478**, 337–342 (2011).
6. Rockström, J. et al. A safe operating space for humanity. *Nature* **461**, 472–475 (2009).
7. Manning, D. A. C. Phosphate minerals, environmental pollution and sustainable agriculture. *Elements* **4**, 105–108 (2008).
8. Gilbert, N. Environment: The disappearing nutrient. *Nature* **461**, 716–718 (2009).
9. Wang, F. et al. Molecular mechanisms of phosphate transport and signaling in higher plants. *Semin. Cell Dev. Biol.* **74**, 114–122 (2018).
10. Guo, T. et al. Advances in rice genetics and breeding by molecular design in China (in Chinese). *Sci. Sin. Vitae.* **49**, 1185–1212 (2019).
11. Ren, M. et al. Phenotypes and molecular mechanisms underlying the root response to phosphate deprivation in plants. *Int. J. Mol. Sci.* **24**, 5107 (2023).
12. Chiou, T. J. & Lin, S. I. Signaling network in sensing phosphate availability in plants. *Annu. Rev. Plant Biol.* **62**, 185–206 (2011).
13. Puga, M. I. et al. Novel signals in the regulation of Pi starvation responses in plants: facts and promises. *Curr. Opin. Plant Biol.* **39**, 40–49 (2017).
14. Wu, P., Shou, H., Xu, G. & Lian, X. Improvement of phosphorus efficiency in rice on the basis of understanding phosphate signaling and homeostasis. *Curr. Opin. Plant Biol.* **16**, 205–212 (2013).
15. Zhang, Z., Liao, H. & Lucas, W. J. Molecular mechanisms underlying phosphate sensing, signaling, and adaptation in plants. *J. Integr. Plant Biol.* **56**, 192–220 (2014).
16. Wang, F. et al. CASEIN KINASE2-Dependent phosphorylation of PHOSPHATE2 fine-tunes phosphate homeostasis in rice. *Plant Physiol.* **183**, 250–262 (2020).
17. Guo, R. et al. Phosphate-dependent regulation of vacuolar trafficking of OsSPX-MFSs is critical for maintaining intracellular phosphate homeostasis in rice. *Mol. Plant* **16**, 1304–1320 (2023).
18. Yang, Z. et al. PROTEIN PHOSPHATASE95 regulates phosphate homeostasis by affecting phosphate transporter trafficking in rice. *Plant Cell* **32**, 740–757 (2020).
19. Lv, Q. et al. SPX4 Negatively regulates phosphate signaling and homeostasis through its interaction with PHR2 in rice. *Plant Cell* **26**, 1586–1597 (2014).
20. Wang, Z. et al. Rice SPX1 and SPX2 inhibit phosphate starvation responses through interacting with PHR2 in a phosphate-dependent manner. *Proc. Natl. Acad. Sci. USA* **111**, 14953–14958 (2014).
21. Ruan, W. et al. Two RING-finger Ubiquitin E3 ligases regulate the degradation of SPX4, An internal phosphate sensor, for phosphate homeostasis and signaling in rice. *Mol. Plant* **12**, 1060–1074 (2019).
22. Zhong, Y. et al. Rice SPX6 negatively regulates the phosphate starvation response through suppression of the transcription factor PHR2. *N. Phytol.* **69**, 385–397 (2018).
23. Shi, J. et al. The paralogous SPX3 and SPX5 genes redundantly modulate Pi homeostasis in rice. *J. Exp. Bot.* **65**, 859–870 (2014).
24. Liu, F. et al. OsSPX1 suppresses the function of OsPHR2 in the regulation of expression of OsPT2 and phosphate homeostasis in shoots of rice. *Plant J.* **62**, 508–517 (2010).
25. Duan, K. et al. Characterization of a sub-family of Arabidopsis genes with the SPX domain reveals their diverse functions in plant tolerance to phosphorus starvation. *Plant J.* **54**, 965–975 (2008).
26. Guo, M. et al. A reciprocal inhibitory module for Pi and iron signaling. *Mol. Plant* **15**, 138–150 (2022).

27. Zhang, G. et al. Brassinosteroid-dependent phosphorylation of PHOSPHATE STARVATION RESPONSE2 reduces its DNA-binding ability in rice. *Plant Cell* **36**, 2253–2271 (2024).

28. Miura, K. et al. The Arabidopsis SUMO E3 ligase SIZ1 controls phosphate deficiency responses. *Proc. Natl. Acad. Sci. USA* **102**, 7760–7665 (2005).

29. Wang, P. et al. Reactive oxygen species: Multidimensional regulators of plant adaptation to abiotic stress and development. *J. Integr. Plant Biol.* **66**, 330–367 (2024).

30. Xia, X. J. et al. Interplay between reactive oxygen species and hormones in the control of plant development and stress tolerance. *J. Exp. Bot.* **10**, 2839–2856 (2015).

31. Garcia-Santamarina, S., Boronat, S. & Hidalgo, E. Reversible cysteine oxidation in hydrogen peroxide sensing and signal transduction. *Biochemistry* **53**, 2560–2580 (2014).

32. Saxena, I., Srikanth, S. & Chen, Z. Cross talk between H_2O_2 and interacting signal molecules under plant stress response. *Front. Plant Sci.* **7**, 570 (2016).

33. Meinhard, M., Rodriguez, P. L. & Grill, E. The sensitivity of ABI2 to hydrogen peroxide links the abscisic acid-response regulator to redox signalling. *Planta* **214**, 775–782 (2002).

34. Meinhard, M. & Grill, E. Hydrogen peroxide is a regulator of ABI1, a protein phosphatase 2C from Arabidopsis. *FEBS Lett.* **508**, 443–446 (2001).

35. Yuan, H. M., Liu, W. C. & Lu, Y. T. CATALASE2 coordinates SA-mediated repression of both auxin accumulation and JA biosynthesis in plant defenses. *Cell Host Microbe* **21**, 143–155 (2017).

36. Mou, Z., Fan, W. & Dong, X. Inducers of plant systemic acquired resistance regulate NPR1 function through redox changes. *Cell* **113**, 935–944 (2003).

37. Tian, Y. et al. Hydrogen peroxide positively regulates brassinosteroid signaling through oxidation of the BRASSINAZOLE-RESISTANT1 transcription factor. *Nat. Commun.* **9**, 1063 (2018).

38. Fu, Z. W. et al. Salt stress-induced chloroplastic hydrogen peroxide stimulates pdTPI sulfenylation and methylglyoxal accumulation. *Plant Cell* **35**, 1593–1616 (2023).

39. Liu, W. C. et al. Coordination of plant growth and abiotic stress responses by tryptophan synthaseβsubunit 1 through modulation of tryptophan and ABA homeostasis in Arabidopsis. *Mol. Plant* **15**, 973–990 (2022).

40. Zhou, H. et al. Rice GLUTATHIONEPEROXIDASE1-mediated oxidation of bZIP68 positively regulates ABA-independent osmotic stress signaling. *Mol. Plant* **15**, 651–670 (2022).

41. Liu, W. C. et al. Sulfenylation of ENOLASE2 facilitates H_2O_2-conferred freezing tolerance in Arabidopsis. *Dev. Cell* **57**, 1883–1898 (2022).

42. Ben et al. Hydrogen peroxide produced by NADPH oxidases increases proline accumulation during salt or mannitol stress in Arabidopsis thaliana. *N. Phytol.* **208**, 1138–1148 (2015).

43. Yun, B. W. et al. S-nitrosylation of NADPH oxidase regulates cell death in plant immunity. *Nature* **478**, 264–268 (2011).

44. Foreman, J. et al. Reactive oxygen species produced by NADPH oxidase regulate plant cell growth. *Nature* **422**, 442–446 (2003).

45. Monshausen, G. B. et al. Ca2+ regulates reactive oxygen species production and pH during mechanosensing in Arabidopsis roots. *Plant Cell* **21**, 2341–2356 (2009).

46. Torres, M. A., Dangl, J. L. & Jones, J. D. Arabidopsis gp91phox homologues AtrbohD and AtrbohF are required for accumulation of reactive oxygen intermediates in the plant defense response. *Proc. Natl. Acad. Sci. USA* **99**, 517–522 (2002).

47. Kwak, J. M. et al. NADPH oxidase AtrbohD and AtrbohF genes function in ROS-dependent ABA signaling in Arabidopsis. *EMBO J.* **22**, 2623–2633 (2003).

48. Miller, G. et al. The plant NADPH oxidase RBOHD mediates rapid systemic signaling in response to diverse stimuli. *Sci. Signal* **2**, ra45 (2009).

49. Denness, L. et al. Cell wall damage-induced lignin biosynthesis is regulated by a reactive oxygen species- and jasmonic acid-dependent process in Arabidopsis. *Plant Physiol.* **156**, 1364–1374 (2011).

50. Hamann, T., Bennett, M., Mansfield, J. & Somerville, C. Identification of cell-wall stress as a hexose-dependent and osmosensitive regulator of plant responses. *Plant J.* **57**, 1015–1026 (2009).

51. Müller, K. et al. The NADPH-oxidase AtrbohB plays a role in Arabidopsis seed after-ripening. *N. Phytol.* **184**, 885–897 (2009).

52. Torres, M. A., Jones, J. D. & Dangl, J. L. Pathogen-induced, NADPH oxidase-derived reactive oxygen intermediates suppress spread of cell death in Arabidopsis thaliana. *Nat. Genet.* **37**, 1130–1134 (2005).

53. Liu, W. C. et al. CATALASE2 functions for seedling postgerminative growth by scavenging H_2O_2 and stimulating ACX2/3 activity in Arabidopsis. *Plant Cell Environ.* **40**, 2720–2728 (2017).

54. Tsukagoshi, H., Busch, W. & Benfey, P. N. Transcriptional regulation of ROS controls transition from proliferation to differentiation in the root. *Cell* **143**, 606–616 (2010).

55. Moller, I. M., Jensen, P. E. & Hansson, A. Oxidative modifications to cellular components in plants. *Annu. Rev. Plant Biol.* **58**, 459–481 (2007).

56. Kim, J. R. et al. Identification of proteins containing cysteine residues that are sensitive to oxidation by hydrogen peroxide at neutral pH. *Anal. Biochem.* **283**, 214–221 (2000).

57. Secco, D. et al. Spatio-temporal transcript profiling of rice roots and shoots in response to phosphate starvation and recovery. *Plant Cell* **25**, 4285–4304 (2013).

58. Naumann, C. et al. Bacterial-type ferroxidase tunes iron-dependent phosphate sensing during Arabidopsis root development. *Curr. Biol.* **32**, 2189–2205 (2022).

59. Mora-Macías, J. et al. Malate-dependent Fe accumulation is a critical checkpoint in the root developmental response to low phosphate. *Proc. Natl. Acad. Sci. USA* **114**, E3563–E3572 (2017).

60. Clúa, J. et al. A CYBDOM protein impacts iron homeostasis and primary root growth under phosphate deficiency in Arabidopsis. *Nat. Commun.* **15**, 423 (2024).

61. Liu, C. et al. The protein phosphatase PC1 dephosphorylates and deactivates CatC to negatively regulate H_2O_2 homeostasis and salt tolerance in rice. *Plant Cell* **35**, 3604–3625 (2023).

62. Ried, M. K. et al. Inositol pyrophosphates promote the interaction of SPX domains with the coiled-coil motif of PHR transcription factors to regulate plant phosphate homeostasis. *Nat. Commun.* **12**, 384 (2021).

63. Zhou, J. et al. Mechanism of phosphate sensing and signaling revealed by rice SPX1-PHR2 complex structure. *Nat. Commun.* **12**, 7040 (2021).

64. Guan, Z. et al. Mechanistic insights into the regulation of plant phosphate homeostasis by the rice SPX2 – PHR2 complex. *Nat. Commun.* **13**, 1581 (2022).

65. Lian, T. et al. Crystal Structure of Tetrameric Arabidopsis MYC2 Reveals the Mechanism of Enhanced Interaction with DNA. *Cell Rep.* **19**, 1334–1342 (2017).

66. Xu, Y., Liu, F., Han, G. & Cheng, B. Genome-wide identification and comparative analysis of phosphate starvation-responsive transcription factors in maize and three other gramineous plants. *Plant Cell Rep.* **37**, 711–726 (2018).

67. David, M. et al. Phytozome: a comparative platform for green plant genomics. *Nucleic Acids Res.* **40**, 1178–1186 (2012).

68. Ma, X. et al. A robust CRISPR/Cas9 system for convenient, high-efficiency multiplex genome editing in monocot and dicot plants. *Mol. Plant* **8**, 1274–1284 (2015).

69. Hiei, Y., Otis, S., Komari, T. & Kumashiro, T. Efficient transformation of rice (Oryza sativa L.) mediated by Agrobacterium and sequence analysis of the boundaries of the T-DNA. *Plant J.* **6**, 271–282 (1994).

70. Noctor, G., Mhamdi, A. & Foyer, C. H. Oxidative stress and anti-oxidative systems: recipes for successful data collection and interpretation. *Plant Cell Environ.* **39**, 1140–1160 (2016).

71. Xiang, D. et al. Root-secreted peptide OsPEP1 regulates primary root elongation in rice. *Plant J.* **107**, 480–492 (2021).

72. Zhou, J. et al. OsPHR2 is involved in phosphate-starvation signaling and excessive phosphate accumulation in shoots of plants. *Plant Physiol.* **146**, 1673–1686 (2008).

73. Hellens, R. P. et al. Transient expression vectors for functional genomics, quantification of promoter activity and RNA silencing in plants. *Plant Methods* **1**, 13 (2005).

74. Malapeira, J. & Mas, P. ChIP-seq analysis of histone modifications at the core of the Arabidopsis circadian clock. *Methods Mol. Biol.* **1158**, 57–69 (2014).

75. Ueguchi-Tanaka, M. et al. Gibberellin insensitive dwarf1 encodes a soluble receptor for gibberellin. *Nature* **437**, 693–698 (2005).

76. Abramson, J. et al. Accurate structure prediction of biomolecular interactions with AlphaFold 3. *Nature* **630**, 493–500 (2024).

77. Pettersen, E. F. et al. UCSF Chimera—a visualization system for exploratory research and analysis. *J. Comput. Chem.* **25**, 1605–1612 (2004).

Acknowledgements

Author contributions

F.M., C.M., and D.X. designed the research. F.M., D.X., R.L., X.S., and Z.B. performed the experiments. F.M., D.X., J.X., Y.W., Y.L., Z.W., X.M., J.P., and C.M. analyzed the data. F.M., D.X., J.P., and C.M. wrote the manuscript.

Competing interests

The authors declare no competing interests.

Additional information

Supplementary information The online version contains supplementary material available at https://doi.org/10.1038/s41467-025-63841-0.

Correspondence and requests for materials should be addressed to Chuanzao Mao.

Peer review information *Nature Communications* thanks Christine Foyer, Tomáš Takáč, and the other anonymous reviewer(s) for their contribution to the peer review of this work. A peer review file is available.

Reprints and permissions information is available at http://www.nature.com/reprints

Publisher's note Springer Nature remains neutral with regard to jurisdictional claims in published maps and institutional affiliations.